Chin. J. Astron. Astrophys. Vol. 3, No. 1, (2003) 49–68
(*http://www.chjaa.org* or *http://chjaa.bao.ac.cn*)

Chinese Journal of
Astronomy and
Astrophysics

Statistical Properties of 6.7 GHz Methanol Maser Sources *

Ye Xu [1,2], Xing-Wu Zheng [3] and Dong-Rong Jiang [2]

[1] National Astronomical Observatories, Chinese Academy of Sciences, Urumqi 830011; xuye@nju.edu.cn
[2] Shanghai Astronomical Observatory, Chinese Academy of Sciences, Shanghai 200030
[3] Department of Astronomy, Nanjing University, Nanjing 210093

Received 2002 August 12; accepted 2002 September 23

Abstract We present a statistical analysis of 482 6.7 GHz methanol maser sources from the available literature, on their maser emission and the characteristics of their associated infrared sources. On the color-color diagram, more than 70% of the objects fall within a very small region ($0.57 \leq [25-12] \leq 1.30$ and $1.30 \leq [60-12] \leq 2.50$). This suggests that 6.7 GHz methanol maser emission occurs only within a very short evolutionary phase during the earliest stage of star formation. The velocity ranges of the masers belong to two main groups: one from 1 to 10 km s^{-1}, and one from about 11 to 20 km s^{-1}. These velocity ranges indicate that the masers are probably associated with both disks and outflows. The correlations between the maser and infrared flux densities, and between the maser and infrared luminosities, suggest that far-infrared radiation is a possible pumping mechanism for the masers which most probably originate from some outer molecular envelopes or disks.

Key words: masers — ISM: molecules — stars: circumstellar matter — stars: formation — ISM: HII regions

1 INTRODUCTION

Newly formed massive stars are obscured by dust, and their clearest signature is often strong maser emission at radio frequencies. Methanol maser emission arises from several transitions, the strongest being the $5_1 - 6_0 A^+$ line at 6.7 GHz, which is the second strongest Galactic maser of any molecule, first reported by Menten (1991) and recognized as typical of Class II masers. Class II methanol masers are always found in regions of recent massive star formation and many of them are associated with known ultra-compact (UC) HII regions — a very early phase in the star formation process. Stars earlier than type B2 also give rise to bright hydroxyl and water masers. However, hydroxyl and water masers can also be found in the later stages of a star's life, and interstellar water masers also occur around young stars later than type B2.

* Supported by the National Natural Science Foundation of China.

Hence, only methanol masers are unique indicators of massive star-forming regions. At present extensive surveys have yielded more than 400 6.7 GHz maser sites (Caswell et al. 1995; van der Walt et al. 1995, 1996; Ellingsen 1996; Lyder 1997; Walsh et al. 1997; Slysh et al. 1999; Szymczak & Kus 2000). The widespread occurrence and high intensity of the 6.7 GHz maser line make it one of the best tracers of star-forming regions at present.

Up to now, there does not seem to have been any systematic statistical study of all the known methanol maser sources. In order to understand better the connection between methanol masers and other phenomena typical of star formation region, such as the associated far-infrared sources, we have investigated the statistical properties of all known 6.7 GHz methanol maser sources and found some interesting results.

2 DESCRIPTION OF THE DATA

We have searched the literature for all known 6.7 GHz methanol maser sources and found a total of 482 objects. Among these, 361 have IRAS identifications. All the data are tabulated in Table 1. The first four columns of Table 1 give the galactic coordinates, name of the associated IRAS source and its 1950 equatorial coordinates. Columns 5 to 7 give the peak radial velocity, the radial velocity range and the peak flux density. Column 8 is the distance. Some of the distances are directly quoted from the references and those that have no published distances are heliocentric kinematic distances, computed from the peak velocities of the 6.7 GHz methanol spectrum using the galactic rotation curve of Wouterloot & Brand (1989), and assuming $R_0 =$ 8.5 kpc and $\Theta_0 = 220\,\mathrm{km\ s^{-1}}$. Column 9 lists the references.

3 DATA ANALYSIS

3.1 Galactic Distribution

The distribution of all known methanol masers in the Galaxy is plotted in Fig. 1. It is seen

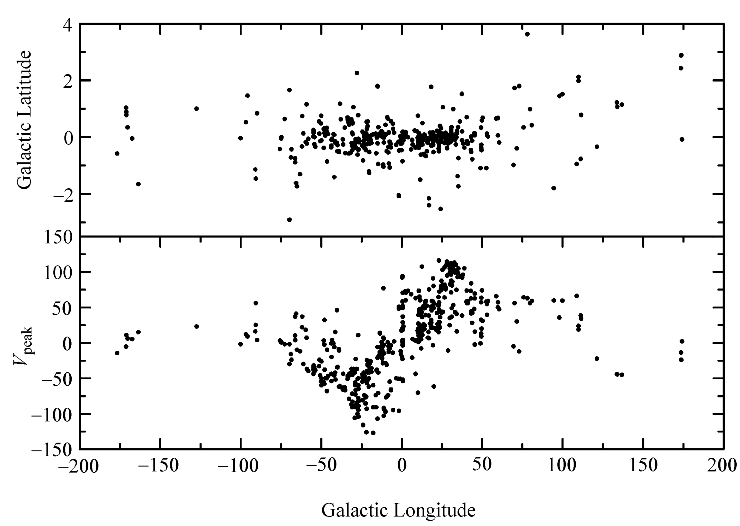

Fig. 1 Distribution in longitude-latitude (upper panel) and longitude-velocity (lower panel) of all known methanol masers in the Galaxy.

that the vast majority lies in the inner galaxy region. The number of masers is about 49% (235/482) in the first quadrant, and 44% (214/482) in the fourth quadrant, i.e., a ratio of 1.1:1.0. This differs slightly from the results of Gaylard & MacLeod (1993) and MacLeod & Gaylard (1992). About 74% (357/482) of the masers lie within $|b| < 0.5°$, and only around 11% (53/482) have galactic latitudes greater than 1°, (the largest is $-12.6°$ for the source 06053–0622).

The distribution in the longitude-velocity diagram shows that the majority of the objects are located in the 'molecular ring' and follow the same distribution as the molecular gas (Dame et al. 2001). This is consistent with the result of van der Walt et al. (1995).

3.2 Infrared Flux Density

Of the 482 6.7 GHz methanol maser sources, 361 have IRAS identifications. Almost 97% (346/361) of the sources satisfy the inequalities $F_{12} < F_{25} < F_{60} < F_{100}$, which characterize the evolutionary stage of young stellar objects, the youngest ones having the steepest spectra, and this also indicates that the emission is mainly produced by cool dust (T $\leq$ 30 K). About 62% (223/361) of the objects have $F_{60} > 500$ Jy and only six objects have $F_{60} < 100$ Jy. It is evident that the 6.7 GHz methanol maser emission is much more likely to occur in sources with high 60 μm fluxes.

3.3 Color-Color Plot

To analyze the infrared properties of the 6.7 GHz methanol masers, we plotted the color-color diagram for the 361 IRAS identified sources. Figure 2 shows the $[25-12]$ vs. $[60-12]$ and $[60-12]$ vs. $[60-25]$ diagrams (here $[i-j] = \log F_i/F_j$). The box on the upper right corner

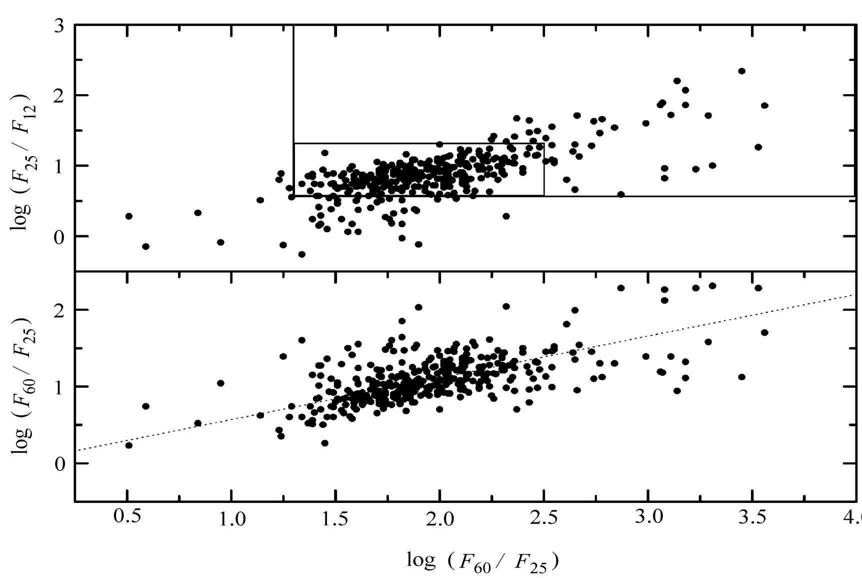

Fig. 2 IRAS color-color diagram for 361 objects. Upper panel: The box in the upper right corner delineates the WC89 criteria for UCHII regions. More than 70% sources fall in a very small region (the central box): $0.57 \leq [25-12] \leq 1.30$ and $1.30 \leq [60-12] \leq 2.50$. Lower panel: The dotted line is the best fit line.

Table 1 Parameters of CH_3OH Spectra

Source Name	IRAS Name	R.A. (1950) ($^{h\ m\ s}$)	DEC (1950) ($^{\circ\ \prime\ \prime\prime}$)	V_{peak} (km s^{-1})	V_{range} (km s^{-1})	S_{peak} (Jy)	D (kpc)	Ref.
121.24 − 0.34	00338+6312	00 33 53.3	63 12 32	−22.4	−27, −21	14	0.9[19]	5
121.24 − 0.34	00338+6312	00 33 53.3	63 12 32	−22.9	−28, −20	10	0.9[19]	3
123.06 − 6.31	00494+5617	00 49 29.2	56 17 37	−29.1	−37, −27	24	2.1[19]	5
123.06 − 6.31	00494+5617	00 49 29.2	56 17 37	−29.0	−31, −27	12	2.1[19]	3
133.72 + 1.22	02219+6152	02 21 54.4	61 52 34	−44.3	−47, −39	5	2.3[11]	3
133.95 + 1.07	02232+6138	02 23 17.7	61 38 58	−44.6	−48, −31	3741	2.2[12]	5
136.84 + 1.14	02455+6034	02 45 30.1	60 34 35	−45.3	−46, −44	24	4.9[3]	3, 5
174.20 − 0.08	05274+3345	05 27 27.6	33 45 37	2.1	0, +6	94	1.8[11]	5
174.20 − 0.08	05274+3345	05 27 27.6	33 45 37	1.8	0, +5	48	1.8[11]	3, 8
173.48 + 2.43	05358+3543	05 35 48.8	35 43 41	−13.6	−16, −11	256	1.8[11]	5
173.63 + 2.87	05379+3550	05 37 59.5	33 50 38		−25, −23	8.2		2
173.70 + 2.89	05382+3547	05 38 15.7	35 47 21	−24.1	−25, −24	7.5	16.5[14]	5
183.35 − 0.58	05480+2545	05 48 04.8	25 45 29	−14.5	−16, −14	19	2.1[17]	3, 5
213.71 − 12.60	06053−0622	06 05 21.7	−06 22 28	10.5	+6, +13	337	0.8[11]	4, 9
213.71 − 12.60	06053−0622	06 05 21.7	−06 22 28	12	+9, +13	166	0.8[11]	5
189.78 + 0.34	06055+2039	06 05 36.6	20 39 30	5.5	+3, +6	17	1.5	5
189.78 + 0.34	06055+2039	06 05 36.6	20 39 30	6	+2, +6	15	1.5	4
189.03 + 0.78	06056+2131	06 05 41.1	21 31 35	10.9	+9, +13	29	1.5[11]	3
189.03 + 0.78	06056+2131	06 05 41.1	21 31 35	9.2	+9, +12	19	1.5[11]	5
189.03 + 0.78	06056+2131	06 05 41.1	21 31 35	9	+8, +10	17	1.5[11]	4
188.95 + 0.89	06058+2138	06 05 53.5	21 39 02	10.4	+8, +12	553	1.5[11]	5
188.95 + 0.89	06058+2138	06 05 53.5	21 39 02	11	+9, +12	495	1.5[11]	4
188.80 + 1.03	06061+2151	06 06 07.3	21 51 12	−5.5	−9, −4	4.8	3.5[14]	5
192.60 − 0.05	06099+1800	06 09 59.1	18 00 10	5.1	+2, +7	64	2.5[11]	5
192.60 − 0.05	06099+1800	06 09 59.1	18 00 10	5	+2, +6	72	2.5[11]	4
196.45 − 1.66	06117+1350	06 11 47.1	13 50 34	15.3	+14, +17	68	4.0[13]	5
196.45 − 1.66	06117+1350	06 11 47.1	13 50 34	15	+13, +16	61	4.0[13]	4
232.62 + 1.00	07299−1651	07 29 54.6	−16 51 48	23	+21, +24	180	2.0	4, 5, 9
232.62 + 1.00	07299−1651	07 29 55.0	−16 51 47		+22, +24	42	2.0	6
259.94 − 0.04	08337−4028	08 33 42.6	−40 28 02	−2		3.8		9
263.25 + 0.52	08470−4243	08 47 00.5	−42 43 15	12	+11, +15	57.3	2.2	6, 9
264.29 + 1.46	08546−4254	08 54 36.2	−42 54 06	9	+6, +10	0.2	1.9	4, 9
269.46 − 1.47	09015−4843	09 01 33.2	−48 43 24	56		4.6	7.7	9
269.16 − 1.14	09018−4816	09 01 50.3	−48 15 57	16	+7, +16	1.4	2.4	4, 9
270.25 + 0.84	09149−4743	09 14 54.1	−47 43 13	4	+3, +5	1.2	1.7	4, 9
284.35 − 0.42		10 22 20.0	−57 37 25	3	+3, +11	2.1	4.7	4
285.26 − 0.05		10 29 35.3	−57 46 44		0, +1	1.7	4.6	8
285.35 − 0.00	10303−5746	10 30 19.3	−57 46 58		0, +1	10.0	4.7	1
285.35 + 0.00	10303−5746	10 30 19.3	−57 46 58	1	−8, +3	8.5	4.7	9
287.36 + 0.64	10460−5811	10 46 03.4	−58 10 58		−3, −1	63.8	4.8	1
287.38 + 0.65	10460−5811	10 46 06.3	−58 11 11	−2	−4, 0	82	4.8	4, 9
290.41 − 2.91	10555−6242	10 55 35.1	−62 42 50	−16	−17, −15	4.0	3.0[9]	9
291.28 − 0.71	11097−6102	11 09 46.7	−61 02 06	−30	−31, −26	107	3.5[9]	4, 9
290.38 + 1.66	11101−5829	11 10 07.7	−58 29 59	−24	−28, −22	2.4	3.0[9]	4, 9
291.57 − 0.43		11 12 52.1	−60 53 02		+9, +13	2.9	7.4	8
291.58 − 0.43		11 12 58.1	−60 53 40	10	+9, +20	3.4	7.3	4
293.83 − 0.75	11298−6155	11 29 48.2	−61 55 49	37	+35, +39	3.8	10.5	9
293.95 − 0.89	11304−6206	11 30 25.0	−62 06 27	41		3.6	10.9	9
294.51 − 1.62	11332−6258	11 33 12.9	−62 58 15		−12, −10	16	1.2/5.9	7
294.52 − 1.62	11332−6258	11 33 15.0	−62 58 13	−10	−14, −9	18	1.2/5.9	4, 9
295.00 − 1.74	11368−6312	11 37 04.8	−63 13 29		−13, −12	26.3	1.5/5.7	7, 9
296.89 − 1.31	11543−6315	11 54 18.9	−63 15 29		+21.5, +23	2.4	9.8	2
298.22 − 0.33		12 07 16.9	−62 33 01	37	+33, +39	1.5	11.5	4
298.26 + 0.74	12091−6129	12 09 08.4	−61 29 37	−30	−31, −29	14	3.8/5.8[9]	9
299.02 + 0.13	12146−6212	12 14 45.6	−62 12 22	18	+18, +20	4.5	9.9	4, 8, 9
300.51 − 0.18	12272−6240	12 27 15.9	−62 40 25	7	+5, +11	4.7	9.3	4, 9
300.51 − 0.18	12272−6240	12 27 16.6	−62 40 30		+7, +9	3.5	9.3	8
300.97 + 1.15	12320−6122	12 32 02.6	−61 23 06	−37	−40, −36	5.0	4.9[9]	4, 9

Table 1 (continued)

Source Name	IRAS Name	R.A. (1950) (^{h} ^{m} ^{s})	DEC (1950) ($^{\circ}$ $'$ $''$)	$V_{\rm peak}$ (km s^{-1})	$V_{\rm range}$ (km s^{-1})	$S_{\rm peak}$ (Jy)	D (kpc)	Ref.
300.97 + 1.15	12320−6122	12 32 02.2	−61 22 59		−38, −36	3.9	4.9[9]	8
301.14 − 0.23	12326−6245	12 32 42.6	−62 45 57	−40	−41, −38	1.5	4.9[9]	4, 9
302.03 − 0.06	12405−6238	12 40 34.5	−62 38 46	−35	−43, −35	9	3.3/6.9[9]	9
302.02 − 0.08	12405−6238	12 40 29.5	−62 39 39		−36, −34	10.8	3.3/6.9[9]	7
305.20 + 0.21		13 07 58.6	−62 18 42	−44	−47, −43	50	4.6/6.9[9]	4
305.21 + 0.21	13079−6218	13 08 01.7	−62 18 45	−38	−42, −34	480	4.4/5.4	4, 9
305.20 + 0.02	13080−6229	13 08 05.7	−62 29 58	−33	−44, −29	52	3.3/6.5	4, 9
305.25 + 0.25		13 08 20.5	−62 16 07	−32	−32, −29	2.3	3.1/6.7	4
305.35 + 0.20	13092−6218	13 09 16.3	−62 18 36	−33	−39, −34	1	3.2/6.6	9
305.36 + 0.15		13 09 22.1	−62 21 25		−37, −33	4.5	6.1	8
305.36 + 0.15		13 09 24.2	−62 21 22	−36	−39, −34	4	6.1	4
305.37 + 0.19		13 09 26.3	−62 19 15	−34	−35, −31	1	6.6	4
305.55 + 0.02	13111−6228	13 11 07.6	−62 28 32	−37	−38, −32	2	3.9/6.0	9
305.81 − 0.25	13134−6242	13 13 30.4	−62 42 44	−39	−40, −36	1.1	4.3/5.6	4, 9
305.89 + 0.00	13140−6226	13 14 02.9	−62 27 26		−35, −31	10.8	3.1/6.8	1
306.33 − 0.34	13180−6245	13 18 07.3	−62 45 01	−24	−25, −22	0.3	2.1/8.0	4, 9
308.74 + 0.55	13374−6130	13 37 25.6	−61 30 19		−52, −40	11.2	4.9/5.7	1
308.92 + 0.12		13 39 35.4	−61 53 47	−55	−56, −53	54		4
309.39 − 0.14		13 43 55.9	−62 03 14	−50	−51, −48	1.2		4
309.92 + 0.48	13471−6120	13 47 11.9	−61 20 19	−60	−65, −53	780	6.3[9]	4, 9
310.13 + 0.75	13484−6100	13 48 24.4	−61 01 30		−58, −54	137.9		1
310.18 − 0.12	13504−6151	13 50 27.9	−61 51 38	3		1.2	11.2	9
311.63 + 0.29	14013−6105	14 01 18.2	−61 05 45	−58	−63, −56	1.9	5.0/8.1[9]	9
311.64 − 0.38	14030−6144	14 03 00.9	−61 43 54		+31, +35	10	15.7[9]	6
311.65 − 0.38	14030−6144	14 03 01.6	−61 44 06	32	+31, +36	15	15.7[9]	4, 9
311.96 + 0.14		14 04 19.7	−61 08 34	−38		0.6	3.1/8.3	4
312.11 + 0.31	14050−6056	14 05 05.2	−60 56 29	−50	−54, −48	4	4.4/7.0	9
312.12 + 0.27	14054−6102	14 05 16.2	−60 58 32		−52, −48	15.0	4.4/7.0	2
312.60 + 0.04	14095−6102	14 09 36.2	−61 02 57	−68	−69, −59	14	6.7[9]	4, 9
312.60 + 0.05	14095−6102	14 09 36.3	−61 02 41		−68	12	6.7[9]	6
313.47 + 0.19	14159−6038	14 16 01.7	−60 38 10		−13, −19	14	0.8/10.9	6
313.47 + 0.19	14159−6038	14 16 00.5	−60 38 01	−10	−16, −3	17	0.8/10.9	4, 9
313.57 + 0.32	14164−6028	14 16 24.4	−60 28 55		−49, −46	149.1	3.8/7.9	1
313.76 − 0.86	14212−6131	14 21 25.0	−61 32 27	−54	−57, −40	40	4.6/7.2	7, 9
314.26 + 0.11	14222−6026	14 22 14.2	−60 26 47	−44		0.4	3.4/8.4	9
314.26 + 0.11	14222−6026	14 22 14.2	−60 26 47		−45, −43	20.7	3.4/8.4	7
316.64 − 0.09	14404−5942	14 30 31.6	−59 42 40	−20	−25, −14	128	1.5/10.6	4, 9
316.40 − 0.30		14 39 27.1	−60 00 22		−6, 4	28	12.4	6
316.36 − 0.36	14394−6004	14 39 23.8	−60 04 33		−6, 8	79.4	12.6	7
316.36 − 0.36	14394−6004	14 39 23.8	−60 04 33	4	+1, +8	96	12.6	4, 9
316.38 − 0.38		14 39 34.7	−60 04 57	−1	−6, +1	38	12.2	4
316.41 − 0.31		14 39 34.8	−60 00 17	−6	−7, −2	10	0.5/11.8	4
316.81 − 0.06	14416−5937	14 41 39.3	−59 36 35	−46	−49, −37	12	3.4/9.0	4, 9
316.81 − 0.07	14416−5937	14 41 38.9	−59 37 11		−46, −42	12	3.4/9.0	6
317.70 + 0.10	14473−5904	14 47 18.9	−59 05 11		−44, −41	32.0	3.1/9.5	1
318.05 + 0.08	14498−5856	14 49 54.5	−58 57 00		−58, −51	4.4	3.8/8.8	9
318.05 + 0.09	14498−5856	14 49 54.0	−58 56 43	−52	−59, −46	4	3.8/8.8	4, 9
318.05 − 1.41	14551−6016	14 55 14.5	−60 16 24	46	+44, +47	7.5	17.5	4, 9
318.78 − 0.15	14557−5849	14 55 43.8	−58 49 27	−34		0.4	2.5/10.3	9
318.95 − 0.20	14567−5846	14 57 03.8	−58 47 01	−35	−39, −31	780	2.6/10.3	4, 9
319.84 − 0.20	15030−5821	15 03 03.0	−58 21 35	−9	−14, −9	0.4	0.7/12.3	4, 9
320.23 − 0.28	15061−5814	15 05 59.3	−58 14 03		−63, −59	24	4.5/8.6	6
320.23 − 0.29	15061−5814	15 06 00.5	−58 14 14	−62	−71, −58	28	4.5/8.6	4, 9
320.12 − 0.50	15061−5828	15 06 06.1	−58 28 44	−11	−12, −9	4.6	0.9/12.2	9
321.03 − 0.50	15122−5801	15 12 02.6	−58 00 50		−63, −60	90.2	4.4/8.8	7
321.06 − 0.52	15122−5801	15 12 16.6	−58 01 12	−62	−69, −54	27	4.4/8.8	9
321.14 − 0.53		15 12 50.9	−57 59 06		−67, −61	7.4	4.5/8.7	8
321.15 − 0.53		15 12 55.3	−57 58 51	−66		9.6	4.7/8.5	4

Table 1 (continued)

Source Name	IRAS Name	R.A. (1950) (^{h} ^{m} ^{s})	DEC (1950) ($^{\circ}$ $'$ $''$)	$V_{\rm peak}$ (km s^{-1})	$V_{\rm range}$ (km s^{-1})	$S_{\rm peak}$ (Jy)	D (kpc)	Ref.
321.71 + 1.17	15100−5613	15 09 58.6	−56 14 19	−44	−45, −38	1.4	3.1/10.2	4, 9
322.16 + 0.63		15 14 46.8	−56 27 34		−65, −53	177	4.4/9.0	6
322.16 + 0.64		15 14 45.7	−56 27 28	−63	−66, −51	211	4.4/9.0	4
323.46 − 0.08	15254−5621	15 25 27.7	−56 21 02	−67	−69, −66	22	4.6/9.1	4, 9
323.74 − 0.26	15278−5620	15 27 52.0	−56 20 40	−51	−59, −46	2860	3.5/10.2	4, 9
324.70 + 0.33		15 31 03.4	−55 18 32		−49, −45	7.1	3.3/10.6	8
324.72 + 0.34		15 31 07.2	−55 17 25	−47	−51, −45	8	3.3/10.6	4
324.92 − 0.56	15360−5554	15 36 02.0	−55 54 19	−79	−80, −78	2.0	5.4/8.5	9
326.47 + 0.69	15394−5358	15 39 28.4	−53 58 28		−51, −37	108.5	3.1/11.1	1
326.64 + 0.60	15408−5356	15 40 45.8	−53 56 38		−44, −36	69.9	3.0/11.2	7
326.66 + 0.59	15408−5356	15 40 53.0	−53 56 31	−43	−45, −37	11	3.0/11.2	9
327.12 + 0.51	15437−5343	15 43 44.3	−53 43 26	−87	−92, −83	90	5.8/8.5	4, 9
327.12 + 0.51	15437−5343	15 43 41.8	−53 43 23		−90, −83	64	5.8/8.5	6
327.29 − 0.58		15 49 16.0	−54 28 14	−37	−49, −37	2.6	2.7/11.6	4
327.40 + 0.44	15454−5335	15 45 30.4	−53 36 10	−83	−85, −72	93	5.4/8.9	4, 9
328.24 − 0.55	15541−5349	15 54 06.1	−53 50 47	−45	−47, −31	400	3.2/11.3	4
328.25 − 0.53	15541−5349	15 54 07.6	−53 49 25	−37	−50, −36	430	3.2/11.3	4, 9
328.81 + 0.63	15520−5234	15 52 00.3	−52 34 22	−44	−47, −42	380	3.1/11.4	4, 9
328.96 + 0.57	15530−5231	15 53 01.2	−52 31 46	−91	−100, −88	2.1	5.8/8.7	9
329.46 + 0.48	15557−5215	15 55 54.2	−52 16 12		−74, −70	17.6	4.7/10.0	7
329.46 + 0.51	15557−5215	15 55 47.9	−52 15 18	−72	−74, −60	10	4.7/10.0	9
330.07 + 1.05	15565−5126	15 56 31.8	−51 26 41		−44, −38	13.2	3.0/11.8	1
329.03 − 0.21		15 56 42.0	−53 04 22	−37	−41, −34	200	2.7/11.9	4
329.03 − 0.20		15 56 40.6	−53 03 58	−42	−48, −40	30	2.7/11.9	4
329.34 + 0.15	15567−5236	15 56 43.5	−52 36 19	−106	−107, −105	10.5	7.8/9.6[9]	9
329.18 − 0.31		15 57 55.5	−53 03 26	−56	−60, −51	13	3.8/10.8	4
329.18 − 0.32		15 57 56.3	−53 03 27		−59, −55	12	3.8/10.8	6
329.60 + 0.10	15584−5230	15 58 17.4	−52 28 12		−62, −58	29.7	4.0/10.7	1
329.40 − 0.46	15596−5301	15 59 40.8	−53 01 13	−67	−73, −63	175	4.4/10.2	4, 9
329.40 − 0.46	15596−5301	15 59 41.1	−53 01 33		−71, −66	122	4.4/10.2	6
332.29 + 2.26	16019−4903	16 02 03.2	−49 04 14		−27, −20	108.8	1.9/13.1	1
330.95 − 0.19	16060−5146	16 06 04.7	−51 47 11	−88	−91, −87	7	5.5/9.4	4, 9
330.96 − 0.18	16060−5146	16 06 05.0	−51 46 44		−89, −87	6.5	5.5/9.4	8
330.88 − 0.38	16065−5158	16 06 34.0	−51 59 00	−73	−73, −56	0.8	4.7/10.2	4, 9
331.13 − 0.24	16071−5142	16 07 10.6	−51 42 33		−91, −84	43	5.7/9.2	6
331.13 − 0.24	16071−5142	16 07 10.8	−51 42 29	−91	−92, −81	28	5.7/9.2	4, 9
331.28 − 0.19	16076−5134	16 07 38.1	−51 34 12	−78	−88, −77	207	5.0/10.0	4, 9
331.54 − 0.07		16 08 22.7	−51 18 10	−84	−87, −80	11	5.3/9.7	4
331.52 − 0.10		16 08 23.2	−51 20 45		−105, −96	35	6.2/8.7	6
331.45 − 0.19	16084−5127	16 08 24.8	−51 27 15		−94, −84	54.4	5.5/9.4	1
331.34 − 0.34	16085−5138	16 08 35.8	−51 38 16		−68, −65	48	4.3/10.6	6
331.34 − 0.35	16085−5138	16 08 37.4	−51 38 32	−65	−73, −61	92	4.3/10.6	4, 9
331.56 − 0.12	16086−5119	16 08 40.6	−51 19 59	−104	−105, −94	47	6.5/8.4	4, 9
332.96 + 0.77	16112−4943	16 11 16.9	−49 43 08	−51		1.1	3.6/11.5	9
332.54 − 0.13	16132−5039	16 13 14.8	−50 39 46	−60	−61, −58	6.3	4.1/11.0	9
332.65 − 0.62	16158−5055	16 15 54.4	−50 56 20	−50	−52, −50	7.1	3.5/11.6	4, 9
333.16 − 0.10	16159−5012	16 15 55.4	−50 12 41	−95	−96, −91	6.3	5.8/9.4	4, 9
333.20 − 0.08		16 16 00.1	−50 10 08	−82	−91, −81	5.8	5.1/10.0	4
333.23 − 0.06		16 16 04.9	−50 08 04	−81	−93, −79	3.8	5.1/10.1	4
332.72 − 0.62		16 16 14.2	−50 53 18	−46	−59, −45	5.4	3.3/11.8	4
333.07 − 0.45		16 17 02.4	−50 31 22	−55	−57, −51	10	3.8/11.3	4
333.12 − 0.43	16172−5028	16 17 12.3	−50 28 40	−49	−57, −45	15	3.5/11.7	4, 9
333.13 − 0.44		16 17 15.5	−50 28 47	−45	−45, −42	3.5	3.5/11.7	4
333.14 − 0.43		16 17 16.7	−50 27 45		−50, −48	17	3.5/11.7	6
333.45 − 0.18		16 17 32.3	−50 04 08		−43, −41	85	3.1/12.1	6

Table 1 (continued)

Source Name	IRAS Name	R.A. (1950) (h m s)	DEC (1950) (° ′ ″)	$V_{\rm peak}$ (km s^{-1})	$V_{\rm range}$ (km s^{-1})	$S_{\rm peak}$ (Jy)	D (kpc)	Ref.
333.47 − 0.17	16175−5002	16 17 34.7	−50 02 45	−42	−49, −36	70	3.1/12.1	4, 9
335.73 + 0.19		16 25 46.0	−48 11 23	−44	−55, −43	74	3.3/12.2	4
335.79 + 0.17		16 26 06.0	−48 09 22	−49	−59, −45	167	3.6/11.9	4
335.59 − 0.29	16272−4837	16 27 15.4	−48 37 20	−47	−56, −44	110	3.5/12.0	4, 9
335.55 − 0.31		16 27 11.3	−48 39 28	−116	119, −110	23	6.9/8.6	4
335.61 − 0.31		16 27 27.8	−48 37 03		−55, −47	68	3.7/11.8	6
336.36 − 0.14	16297−4757	16 29 47.9	−47 57 28	−74	−81, −70	21	4.8/10.8	4, 9
336.36 − 0.15	16297−4757	16 29 50.9	−47 57 46		−81, −73	21	4.8/10.8	6
336.41 − 0.26		16 30 30.7	−48 00 10	−85.6	−86, −85	8	5.3/10.3	4
336.43 − 0.26	16306−4758	16 30 37.6	−47 59 19	−93	−95, −86	46	5.6/9.9	4, 9
336.83 + 0.02		16 31 00.1	−47 30 20		−77, −75	32	5.0/10.7	6
336.83 + 0.02		16 31 00.6	−47 30 20	−77		16	5.0/10.7	4
336.86 − 0.01	16313−4729	16 31 11.2	−47 29 39	−76	−82, −68	34	4.9/10.7	4, 9
336.02 − 0.82	16313−4840	16 31 23.4	−48 40 06	−54	−55, −39	350	3.9/11.7	9
336.01 − 0.82	16313−4840	16 31 21.8	−48 40 51		−55, −39	410.0	3.9/11.7	1
336.99 − 0.03	16318−4724	16 31 51.9	−47 25 03	−126	−127, −116	38	7.6/8.1	4, 9
337.00 − 0.02		16 31 50.6	−47 24 29		−126	28		6
336.83 − 0.38	16327−4746	16 32 44.0	−47 46 23		−27, −22	41.5	2.2/13.5	1
337.62 − 0.06	16344−4658	16 34 29.4	−46 58 57	−42	−54, −38	21	3.3/12.4	4, 9
338.28 + 0.54		16 34 29.8	−46 05 00	−57	−59, −56	5	4.1/11.7	4
337.63 − 0.08		16 34 38.7	−46 58 53	−57	−63, −54	13	4.1/11.6	4
337.71 − 0.06	16348−4654	16 34 49.6	−46 54 43	−55	−58, −43	145	4.0/11.7	4, 9
338.00 + 0.13		16 35 09.8	−46 34 12	−32	−36, −31	4	2.7/13.0	4
337.40 − 0.41	16351−4722	16 35 09.9	−47 22 22		−39.5	57	3.2/12.5	6
337.41 − 0.41	16351−4722	16 35 09.8	−47 22 07	−40	−43, −36	67	3.2/12.5	4, 9
338.08 + 0.02	16359−4635	16 35 58.8	−46 34 54		−54, −43	18	3.9/11.8	6
338.08 + 0.02	16359−4635	16 35 58.2	−46 35 28	−53	−54, −30	18	3.9/11.8	4, 9
338.47 + 0.29		16 36 18.6	−46 06 35	−30	−35, −29	0.7	2.6/13.2	4
338.47 + 0.29		16 36 19.2	−46 06 50		−46, −43	−1.4	2.6/13.2	8
338.92 + 0.55		16 36 54.8	−45 36 14	−62	−68, −59	71	4.4/11.5	4
338.93 + 0.55		16 36 58.0	−45 35 54		−64, −61	64	4.4/11.5	6
338.44 + 0.06	16371−4617	16 37 11.6	−46 17 22	−38	−42, −34	28	3.1/12.7	9
338.43 + 0.05	16371−4617	16 37 12.0	−46 17 49		−31, −29	35.4	3.1/12.7	1
337.92 − 0.48		16 37 29.7	−47 02 12		−39, −37	29		6
337.92 − 0.46	16374−4701	16 37 25.0	−47 01 21	−38	−41, −36	47	3.1/12.7	4, 9
338.93 + 0.39	16376−4542	16 37 39.5	−45 42 38	−26	−34, −22	0.68	2.4/13.5	9
338.46 − 0.25	16381−4629	16 38 36.1	−46 28 38	−50	−57, −49	83	3.8/12.0	4, 9
338.46 − 0.25	16381−4629	16 38 36.5	−46 28 37		−53, −49	62	3.8/12.0	6
338.87 − 0.08		16 39 28.7	−46 03 38	−41	−42, −38	19	3.3/12.5	4
338.88 − 0.08		16 39 29.4	−46 03 05		−41	14	3.3/12.5	6
338.93 − 0.06		16 39 36.5	−46 00 05	−42	−44, −42	12	3.4/12.5	4
339.62 − 0.12	16424−4531	16 42 26.5	−45 31 18	−36	−39, −30	83	3.1/12.8	4, 9
339.62 − 0.13		16 42 29.8	−45 31 43		−38, −32	81	3.1/12.8	7
340.25 − 0.05	16445−4459	16 44 30.1	−44 59 54	−127	−134, −120	10	7.1/8.9	9
340.05 − 0.24	16445−4516	16 44 35.2	−45 16 24	−60	−63, −46	42	4.4/11.6	4, 9
340.06 − 0.25	16445−4516	16 44 36.9	−45 16 27		−61, −59	44	4.4/11.6	6
339.97 − 0.53	16455−4531	16 45 32.7	−45 31 24	−91	−105, −88	40	5.6/10.3	9
340.79 − 0.10		16 46 38.4	−44 37 19	−107	−112, −88	242	6.2/9.8	4
339.68 − 1.21	16474−4610	16 47 25.0	−46 10 59	−21	−41, −21	70	2.1/13.9	4, 9
339.68 − 1.21	16474−4610	16 47 26.2	−46 11 12		−38, −21	57	2.1/13.9	6
341.27 + 0.07		16 47 40.3	−44 08 38		−74, −70	5.1	5.1/11.0	8
341.28 + 0.06		16 47 43.9	−44 08 41	−74	−77, −66	5.5	5.1/11.0	4
339.88 − 1.26	16484−4603	16 48 24.8	−46 03 34	−39	−45, −27	1820	3.3/12.7	4, 9
341.22 − 0.21		16 48 42.1	−44 21 53	−38	−50, −35	167	3.3/12.8	4
342.36 + 0.10	16513−4316A	16 51 23.6	−43 16 51	−91	−92, −88	1.1	5.8/10.4	9
342.36 + 0.10	16513−4316A	16 51 23.6	−43 16 51	−42		0.4	3.7/12.5	9
342.36 + 0.10	16513−4316A	16 51 23.6	−43 16 51	−6	−16, −2	0.7	0.8/15.4	9
345.01 + 1.79	16533−4009	16 53 19.7	−40 09 46	−18	−24, −15	508	2.2/14.2	4, 9
345.01 + 1.80	16533−4009	16 53 18.9	−40 09 29	−13	−15, −10	31	1.7/14.7	4

Table 1 (continued)

Source Name	IRAS Name	R.A. (1950) ($^{h\ m\ s}$)	DEC (1950) ($^{\circ\ \prime\ \prime\prime}$)	$V_{\rm peak}$ (km s^{-1})	$V_{\rm range}$ (km s^{-1})	$S_{\rm peak}$ (Jy)	D (kpc)	Ref.
343.93 + 0.12		16 56 39.1	−42 02 58		+11, +15	12		6
343.91 + 0.11	16566−4204	16 56 38.7	−42 02 58	14	+7, +19	11	19.1	4, 9
344.41 + 0.05		16 58 34.0	−41 43 15		−71, −72	15	6.3/12.8	6
344.42 + 0.05	16586−4142	16 58 37.1	−41 42 36	−71	−73, −63	16	5.2/11.2	4, 9
344.58 − 0.02	16594−4137	16 59 26.2	−41 37 36	1	−5, 2	3.4	16.5	4, 9
344.22 − 0.57	17006−4215	17 00 33.8	−42 14 35		−27, −19	101	2.3/14.0	6
344.23 − 0.57	17006−4215	17 00 35.0	−42 14 29	−20	−33, −16	118	2.3/14.0	4, 9
345.51 + 0.35	17008−4040	17 00 54.2	−40 40 18	−18	−23, −11	174	2.3/14.2	4, 9
345.00 − 0.22	17016−4124	17 01 38.5	−41 24 59	−22	−32, −20	448	2.6/13.9	4, 9
345.80 + 0.05	17031−4037	17 03 06.7	−40 37 02	−10	−13, −8	1.6	1.4/15.1	9
346.48 + 0.13		17 04 54.7	−40 01 41		−20, −18	5.6	1.6/14.9	8
346.48 + 0.13		17 04 55.0	−40 01 40	−11	−12, −5	2.9	1.6/14.9	4
346.52 + 0.12		17 05 05.5	−40 00 15	−2	−2, 0	0.9	0.3/16.2	4
346.52 + 0.09	17052−4001	17 05 13.4	−40 01 25	6		1.8	17.7	4, 9
345.41 − 0.95	17059−4132	17 06 04.9	−41 32 04	−15	−19, −13	2.8	2.0/14.5	4, 9
347.58 + 0.21	17079−3905	17 07 59.5	−39 05 58	−103	−104, −95	2.7	6.5/10.1	4, 9
347.63 + 0.21		17 08 09.6	−39 03 36	−92	−93, −89	11.5	6.2/10.4	4
347.63 + 0.15		17 08 23.9	−39 05 50		−97, −91	14	6.4/10.2	6
347.63 + 0.15		17 08 24.8	−39 06 00	−97	−98, −96	18	6.4/10.2	4
347.82 + 0.02		17 09 32.1	−39 01 17	−25	−26, −23	3.4	3.2/13.4	4
347.86 + 0.02		17 09 39.1	−38 59 16	−29	−38, −23	7.2	3.5/13.1	4
347.91 + 0.05	17096−3856	17 09 39.4	−38 56 02	−28	−31, −27	5.3	3.4/13.2	4, 9
347.87 + 0.01		17 09 41.7	−38 59 13		−29	6	3.5/13.1	6
348.89 + 0.09		17 12 27.6	−38 06 50		−77, −74	5.7	5.9/10.8	8
348.88 + 0.10		17 12 24.7	−38 06 49	−75	−77, −70	7.7	5.9/10.8	4
349.09 + 0.11		17 12 58.4	−37 56 20		−77, −76	21	5.9/10.8	6
349.07 − 0.02		17 13 25.5	−38 02 07	7	+6, +16	1.9	18.5	4
349.10 + 0.11	17130−3756	17 13 00.5	−37 56 19	77	−83, −74	30	7.5/12.2[9]	4, 9
348.89 − 0.19	17136−3816	17 13 37.2	−38 16 16	1		2	16.9	4, 9
350.02 + 0.43	17143−3700	17 14 23.8	−36 59 53		−37, −23	5.0	4.0/12.7	8
350.01 + 0.43	17143−3700	17 14 22.4	−37 00 18	−31	−37, −29	6	4.0/12.7	4, 9
348.24 − 0.98	17149−3916	17 14 56.4	−39 16 02	−12		1	1.9/14.7	9
348.55 − 0.97	17158−3901	17 15 51.1	−39 00 29		−23, −9	40.5	2.1/14.6	8
348.55 − 0.98	17158−3901	17 15 53.0	−39 00 53	−13	−23, −7	74	2.1/14.6	4, 9
350.10 + 0.09	17160−3707	17 16 02.9	−37 07 48	−74	−76, −60	41	6.0/10.7	4, 9
351.16 + 0.70	17165−3554	17 16 36.5	−35 54 39	−5	−7, −2	11	1.7[11]	4, 9
350.34 + 0.10	17166−3656	17 16 39.1	−36 55 58		−67, −61	26.9	5.8/10.9	7
350.33 + 0.10	17166−3656	17 16 40.4	−36 56 14	−66	−67, −56	12	5.8/10.9	9
348.70 − 1.04		17 16 37.1	−38 55 31	−3	−17, −3	60	0.6/16.1	4
348.72 − 1.04	17167−3854	17 16 38.9	−38 54 31	−8	−9, −6	90	1.4/15.3	4, 9
351.42 + 0.65	17175−3544	17 17 32.4	−35 44 04	−10	−12, −7	3300	1.7[11]	4, 9
351.44 + 0.66		17 17 33.6	−35 42 11	−3	−14, +1	16	0.7/16.1	4
350.69 − 0.50	17200−3658	17 20 08.2	−36 58 54		−16, −13	31.3	2.5/14.3	1
352.08 + 0.16		17 21 20.6	−35 27 55	−67	−70, −64	2.3	6.2/10.7	4
352.11 + 0.17		17 21 22.8	−35 26 12	−55	−60, −53	5.8	5.8/11.1	4
351.58 − 0.35	17220−3609	17 22 02.5	−36 09 51		−97, −91	47	6.8/10.0	6
351.58 − 0.35	17220−3609	17 22 03.2	−36 10 09	−95	−100, −87	63	6.8/10.0	4, 9
351.78 − 0.54	17233−3606	17 23 20.7	−36 06 45	2	−9, +3	225	17.4	4, 12
353.46 + 0.56	17234−3405	17 23 33.2	−34 05 53	−50	−53, −50	13	5.9/11.0	4, 9
353.45 + 0.54		17 23 35.7	−34 06 54		−52, −49	10		6
352.51 − 0.15	17238−3516	17 23 48.5	−35 17 13		−54, −49	6.5	5.7/11.2	8
352.52 − 0.16	17238−3516	17 23 51.4	−35 17 06	−51	−54, −49	6.3	5.7/11.2	4, 9
352.60 − 0.18	17242−3513	17 24 12.2	−35 13 37	−96	−96, −80	1.7	7.0/9.9	9
352.12 − 0.93	17258−3602	17 25 55.7	−36 02 20		−18, −7	20.1	2.5/14.3	1
353.22 − 0.24	17260−3445	17 26 05.6	−34 45 06	−16		0.4	3.4/13.5	9
354.62 + 0.47	17269−3312	17 26 59.8	−33 11 34	−23	−27, −13	216	4.6/12.3	4, 9
353.41 − 0.36	17271−3439	17 27 06.6	−34 36 30	−20	−23, −19	90	3.9/13.0	4, 9
352.63 − 1.07	17278−3541	17 27 52.4	−35 41 57	−3	−7, 7	180	0.9/16.0	9

Table 1 (continued)

Source Name	IRAS Name	R.A. (1950) (^{h} ^{m} ^{s})	DEC (1950) ($^{\circ}$ $'$ $''$)	$V_{\rm peak}$ (km s^{-1})	$V_{\rm range}$ (km s^{-1})	$S_{\rm peak}$ (Jy)	D (kpc)	Ref.
352.64 − 1.09	17278−3541	17 27 58.8	−35 41 56		−8, 7	143.2	0.9/16.0	7
354.72 + 0.30	17279−3311	17 27 57.2	−33 11 54	94	+92, +103	18	8.8[9]	9
354.74 + 0.29	17279−3311	17 28 03, 6	−33 11 49		+91, +95	21.0	8.8[9]	7
355.34 + 0.15	17302−3245	17 30 12.2	−32 45 56	20	+5, +21	9.6	24.4[9]	4, 9
356.66 − 0.27	17352−3153	17 35 14.2	−31 53 07	−54	−57, −45	9	7.0/9.9	4, 9
356.66 − 0.27	17352−3153	17 35 15.4	−35 53 17		−56, −45	9.6	7.0/9.9	8
357.96 − 0.17	17381−3043	17 38 06.8	−30 44 19		−6, +1	39.6	2.4/14.6	1
359.14 + 0.03	17402−2938	17 40 14.2	−29 38 03	−4	−7, 0	17	4.8/12.2	4, 9
358.38 − 0.48	17403−3032	17 40 22.3	−30 32 35	2	−6, +13	21	21.2	9
358.38 − 0.48	17403−3032	17 40 22.3	−30 32 35		−1, +3	25.0	21.2	7
359.44 − 0.10		17 41 29.1	−29 26 59	−52.0	−53, −45	26.8	8.2/8.8	10
359.44 − 0.10		17 41 29.1	−29 26 59	−52	−57, −45	27	8.2/8.8	4
359.61 − 0.24		17 42 27.2	−29 22 18	20	+14, +27	48		4
359.62 − 0.24		17 42 27.8	−29 21 58	22.5	+14, +27	88.7		10
0.50 + 0.18	17429−2823	17 42 55.1	−28 23 56	1	−11, +2	10	3.0/14.0	9
0.21 − 0.00		17 42 56.8	−28 44 17	49.2	+41, +50	3.5	8.4/8.6	10
0.22 − 0.01	17430−2844	17 43 00.3	−28 44 03	50	+42, +50	3.2	8.4/8.6	9
0.53 + 0.18	17430−2822	17 43 00.0	−28 22 22	0.0	−11, +3	7	17.0	3
0.53 + 0.18	17430−2822	17 43 00.0	−28 22 22	3		0.4	5.2/11.8	9
0.53 + 0.18	17430−2822	17 43 00.0	−28 22 22		−11, +2	11.9	17.0	7
0.38 + 0.04	17432−2835	17 43 11.3	−28 34 37	37	+35, +40	0.7	8.2/8.8	4, 9, 10
0.39 − 0.03		17 43 29.6	−28 36 02	28.7	+22.5, +31	5.8	8.1/8.9	10
0.81 + 0.18	17436−2807	17 43 41.5	−28 06 31	4	+2, +5	5.4	4.8/12.2	9
0.84 + 0.18		17 43 45.1	−28 06 26	3.5	+2, +4	8.1	4.5/12.5	10
0.83 + 0.19	17436−2806	17 43 41.0	−28 06 31	4.0	+3, +5	20	4.8/12.2	3
0.84 + 0.19	17436−2806	17 43 42.3	−28 06 24		+3, +4	8.9	4.8/12.2	1
0.30 − 0.20	17439−2845	17 43 57.7	−28 45 55		+14, +21	29.5	8.0/9.0	1
0.31 − 0.20	17439−2845	17 43 58.2	−28 45 15	18	+14, +27	38	8.0/9.0	9, 10
0.60 − 0.05	17440−2825	17 44 04.8	−28 25 49	49.5	+47, +53	66	8.2/8.8	3
0.64 − 0.04	17440−2823	17 44 08.9	−28 23 29	49	+48, +53	69	8.1/8.6	4, 9, 10
0.66 − 0.03		17 44 09.2	−28 21 57	70.4	+70, +73	18	8.3/8.7	4
0.66 − 0.04		17 44 10.5	−28 22 33	52.0	+48, +56	3.0	8.3/8.7	10
359.97 − 0.46	17441−2910	17 44 09.8	−29 10 59	23	+20, +23	1	9.8[9]	4, 9, 10
0.65 − 0.06		17 44 13.8	−28 23 41	51.0	+49, +52	3.4	8.3/8.7	10
0.65 − 0.05		17 44 11.4	−28 23 22	48.0	+46, +49	31.7	8.3/8.7	10
0.65 − 0.05		17 44 11.0	−28 23 23	48	+46, +52	33	8.3/8.7	4
0.67 − 0.03	17441−2822	17 44 09.8	−28 22 05	58.2	+55, +59	4.5	8.2/8.8	10
0.67 − 0.03	17441−2822	17 44 09.8	−28 22 05	72.2	+68, +73	33.7	8.2/8.8	10
0.67 − 0.03	17441−2822	17 44 09.8	−28 22 05	70.4	+70, +73	18	8.2/8.8	9
0.67 − 0.03	17441−2822	17 44 10.8	−28 21 40	69.2	+57, +77	24	8.2/8.8	4
0.67 − 0.04	17441−2822	17 44 12.0	−28 22 02	60.4	+58, +62	2.1	8.2/8.8	10
0.68 − 0.03	17441−2822	17 44 11.1	−28 21 12	73.4	+70, +77	4.4	8.2/8.8	10
0.69 − 0.04	17443−2821	17 44 14.7	−28 20 52	68.6	+64, +72	32	8.2/8.8	4, 9
0.70 − 0.04	17443−2821	17 44 16.2	−28 20 30	68.5	+64, +75	26	8.2/8.8	11
1.13 − 0.11	17455−2800	17 45 32.3	−28 00 43	−21	−21, −15	2.6	10.0[9]	9
358.26 − 2.05	17463−3128	17 46 21.3	−31 28 20	5.2	+1, +7	31		3
358.27 − 2.08	17463−3128	17 46 27.0	−31 28 38		+1, +7	16.7		1
0.55 − 0.85	17470−2853	17 47 04.4	−28 53 39	14	+8, +20	68	7.5/9.5	4, 9
2.14 + 0.01		17 47 28.1	−27 05 02	63	+53, +65	10	7.6/9.3	4
2.61 + 0.13	17480−2636	17 48 04.7	−26 36 57	3	+2, +20	52	2.0/15.0	9
2.55 + 0.18	17480−2636	17 47 44.4	−26 38 52		+2, +7	63.7	2.0/15.0	7
3.91 + 0.00		17 51 33.1	−25 34 16	17	+17, +24	2.1	4.7/12.3	4
5.90 − 0.43	17574−2403	17 57 36.9	−24 04 22	10	−1, +13	8	2.6[9]	4, 9
6.55 − 0.10	17577−2320	17 57 46.9	−23 20 19	13	0, +15	1.6	16.7[9]	9
6.55 − 0.10	17577−2320	17 57 46.9	−23 20 19		0, +2	5.5	16.7[9]	7
6.78 − 0.27	17589−2312	17 58 56.2	−23 13 53		+14, +30	78.9	4.5/12.4	1
6.79 − 0.26	17589−2312	17 58 54.7	−23 12 39	26.9	+15, +30	84	4.5/12.4	3
8.14 + 0.23	17599−2148	17 59 59.9	−21 48 12	20	+18, +22	12	4.2[9]	9
8.13 + 0.22	17599−2148	18 00 01.2	−21 49 11		+19, +21	14.6	4.2[9]	8

Table 1 (continued)

Source Name	IRAS Name	R.A. (1950) (h m s)	DEC (1950) (° ′ ″)	$V_{\rm peak}$ (km s^{-1})	$V_{\rm range}$ (km s^{-1})	$S_{\rm peak}$ (Jy)	D (kpc)	Ref.
10.10 + 0.75	18021−1950	18 02 12.0	−19 50 52	2		0.4	0.4/16.3	9
8.67 − 0.35	18032−2137	18 03 14.6	−21 37 54	39		5.6	6.2[9]	9
8.67 − 0.36		18 03 18.6	−21 37 45	39		5.6	4.8/11.9	4
8.68 − 0.37		18 03 22.6	−21 37 24	43	+41, +46	148	4.8/11.9	4
9.62 + 0.20	18032−2032	18 03 14.7	−20 32 08	1	−4, +9	5090	16.5	9
9.62 + 0.20	18032−2032	18 03 16.0	−20 31 53	1	−4, +9	5090	16.5	4
9.99 − 0.03	18048−2019	18 04 53.1	−20 19 04	47	+40, +52	28	50[20]	9
9.98 − 0.04	18048−2019	18 04 55.0	−20 19 58		+40, +48	35.4	5.0/11.8	7
10.48 + 0.03	18056−1952	18 05 39.7	19 51 52	65	+58, +66	16	7.3[9]	4
10.47 + 0.03	18056−1952	18 05 38.7	−19 52 34	73.4	+70, +75	9.8	7.3[9]	5
10.47 + 0.03	18056−1952	18 05 40.0	−19 52 24	75	+58, +77	61	7.3[9]	4, 9
10.44 + 0.01	18056−1954	18 05 41.3	−19 54 25	73	+57, +79	16.5	5.9/10.8	9
10.45 − 0.02		18 05 47.0	−19 55 01	73.2	+68, +79	25	5.9/10.8	4
10.30 − 0.15	18060−2005	18 05 57.9	−20 06 26	10.6	+4, +18	131	6.0[9]	3
10.31 − 0.15	18060−2005	18 06 00.3	−20 05 57	11	+2, +21	80	6.0[9]	9
10.33 − 0.17	18060−2005	18 06 06.7	−20 05 34		+4, +17	108.7	1.9/14.8	7
10.88 + 0.13	18061−1927	18 06 09.6	−19 27 56	16.8	+14, +18	4.5	2.6/14.1	5
10.32 − 0.26	18064−2008	18 06 26.0	−20 08 42	39.0	+9, +40	9	4.5/12.2	3
10.96 + 0.01	18067−1927	18 06 44.2	−19 27 35		+23, +26	20.2	3.3/13.4	7
10.96 + 0.02	18067−1927	18 06 43.9	−19 27 03	23.9	+23, +25	15	3.3/13.4	5
10.96 + 0.02	18067−1927	18 06 43.9	−19 27 03	25		18	3.3/13.4	9
11.03 + 0.06	18067−1921	18 06 42.4	−19 22 03	20	+15, +21	0.7	2.9/13.8	4, 9
10.62 − 0.32	18072−1954	18 07 16.2	−19 54 49	−8	−13, +1	3.4	18.9	9
10.62 − 0.32	18072−1954	18 07 16.2	−19 54 49	−8.0	−9, 0	3.4	18.9	5
10.63 − 0.34		18 07 21.4	−19 54 39	−8	−13, +1	3.4	18.9	4
10.63 − 0.38	18075−1956	18 07 31.0	−19 56 19	5	−10, +7	3.6	6.5[9]	4, 9
12.89 + 0.49	18089−1732	18 08 56.4	−17 32 14	39	+27, +43	93	4.1/12.5	4, 9
12.89 + 0.49	18089−1732	18 08 56.4	−17 32 14	38.9	+29, +40	61	4.1/12.5	5
12.03 − 0.03	18090−1832	18 09 06.3	−18 32 43	108	+105, +113	82	6.7/10.0	4, 9
12.03 − 0.03	18090−1832	18 09 05.7	−18 32 42	107.4	+105, +112	77	6.7/10.0	5
11.91 − 0.11		18 09 08.0	−18 41 15	36	+33, +37	2.6	4.0/12.6	4
11.90 − 0.14	18092−1842	18 09 15.2	−18 42 21	43	+39, +44	67	4.4/12.2	4
11.90 − 0.14	18092−1842	18 09 13.7	−18 42 20	42.6	+39, +44	49	4.4/12.2	5
11.94 − 0.15	18094−1840	18 09 20.3	−18 40 51	48	+45, +49	2.3	4.7/11.9	4, 9
11.95 − 0.16	18094−1840	18 09 24.7	−18 40 23	46.8	+46, +49	2.3	4.7/11.9	5
12.25 − 0.05	18096−1821	18 09 37.2	−18 21 08	48.7	+47, +54	9.2	4.7/11.9	5
12.21 − 0.10	18097−1825*A*	18 09 44.0	−18 25 09	20	+19, +21	15	16.1[9]	4, 9
12.20 − 0.11	18097−1825*A*	18 09 44.1	−18 25 36	17	+16, +23	3.7	16.1[9]	4
12.20 − 0.12		18 09 46.4	−18 25 55	26	+26, +32	3.5	3.3/13.4	4
12.22 − 0.11	18097−1825	18 09 47.4	−18 25 06	19.1	+15, +30	7.9	2.6/14.0	5
11.99 − 0.28	18099−1841	18 09 55.6	−18 41 32	60	+55, +62	1.8	5.2/11.4	9
11.99 − 0.28	18099−1841	18 09 55.6	−18 41 32	60.2	+60, +61	2.3	5.2/11.4	5
12.63 − 0.02	18102−1800	18 10 16.7	−18 00 26	24.0	+20, +26	11	2.9/13.6[3]	3
12.63 − 0.02	18102−1800	18 10 16.7	−18 00 26	24.4	+22, +27	13	2.9/13.6[3]	5
12.71 − 0.13	18108−1759	18 10 52.4	−17 59 36	57.7	+50, +61	264	5.0/11.6	5
12.68 − 0.18		18 10 59.6	−18 02 29	52	+50, +62	544	4.8/11.8	4
11.94 − 0.62	18110−1854	18 11 04.1	−18 54 21	32	+30, +44	47	3.8/12.9	4, 5, 9
12.93 − 0.08	18111−1746	18 11 07.0	−17 46 32	58.7	+58, +61	8.3	5.0/11.5	5
13.18 + 0.05	18111−1729	18 11 10.1	−17 29 36	48.5	+48, +49	6.4	4.5/12.0	5
12.91 − 0.26	18117−1753	18 11 43.8	−17 53 04	39	+35, +47	317	3.7[16]	4, 9
12.91 − 0.26	18117−1753	18 11 43.7	−17 53 01	39.8	+35, +41	242	3.7[16]	5
13.71 − 0.08	18126−1705	18 12 41.1	−17 05 33	51.9	+42, +52	3.4	4.6/11.9	5
14.10 + 0.09	18128−1640	18 12 51.1	−16 39 53	15.3	+5, +16	200	15[16]	3
14.10 + 0.09	18128−1640	18 12 51.8	−16 40 01	15.1	+4, +17	135	15[16]	5
11.50 − 1.49	18134−1942	18 13 24.6	−19 42 25	7	+5, +17	160	1.1/15.5	9
11.51 − 1.50	18134−1942	18 13 28.3	−19 42 25		+6, +17	247.7	1.1/15.5	7
11.51 − 1.50	18134−1942	18 13 28.3	−19 42 25	6.2	+4, +17	116	1.1/15.5	5
14.44 − 0.06	18141−1626	18 14 06.2	−16 26 31	27.0	+26, +28	3.0	3.0/13.4	5

Table 1 (continued)

Source Name	IRAS Name	R.A. (1950) (h m s)	DEC (1950) (° ′ ″)	V_{peak} (km s^{-1})	V_{range} (km s^{-1})	S_{peak} (Jy)	D (kpc)	Ref.
14.61 + 0.01	18141−1615	18 14 09.0	−16 15 47	23	+19, +35	2.3	2.8/13.6	9
14.61 + 0.01	18141−1615	18 14 09.0	−16 15 47	24.8	+22, +28	2.9	2.8/13.6	5
13.66 − 0.60	18144−1723	18 14 29.8	−17 23 23	51.0	+47, +52	33	4.4[20]	5
18.34 + 1.77	18151−1208	18 15 09.0	−12 08 33	28.2	+27, +29	72	2.6/13.5[3]	3
18.34 + 1.77	18151−1208	18 15 09.0	−12 08 33	27.7	+27, +29	65	2.6/13.5[3]	5
18.33 + 1.76	18151−1208	18 15 10.3	−12 08 60		+27, +29	46.1	2.6/13.5[3]	1
15.08 − 0.12	18155−1554	18 15 34.8	−15 54 50	45.8	+45, +46	3.1	4.2/12.3	5
14.33 − 0.64	18159−1648	18 15 59.6	−16 48 55	21	+21, +24	0.4	2.5[20]	9
15.03 − 0.68	18174−1612	18 17 31.6	−16 13 02	21	+21, +24	39	2.5[18]	4, 9
15.03 − 0.67	18174−1612	18 17 29.3	−16 12 48	20.9	+20, +23	19	2.5[18]	5
15.66 − 0.50	18181−1534	18 18 06.7	−15 34 36	−3.4	−5, −2	33	16.9	5
16.59 − 0.05	18182−1433	18 18 18.5	−14 33 16	59	+52, +69	21	4.7/11.6	4, 9
16.58 − 0.05	18182−1433	18 18 16.8	−14 33 19	61.6	+56, +69	24	4.7/11.6	5
16.36 − 0.21	18184−1449	18 18 25.6	−14 49 34	52.1	+49, +53	10	4.3/12.0	5
17.02 − 0.09	18193−1411	18 19 18.9	−14 11 26	90.8	+90, +91	1.3	5.8/10.5	5
17.64 + 0.16	18196−1331	18 19 36.5	−13 31 38	21		25	2.0[11]	4
17.64 + 0.15	18196−1331	18 19 37.3	−13 31 45		+21	22	2.0[11]	6
17.64 + 0.15	18196−1331	18 19 37.3	−13 31 45	20.5	+20, +21	20	2.0[11]	5
18.07 + 0.08	18207−1311	18 20 42.5	−13 11 01	55.2	+45, +57	3.9	4.3/11.8	5
18.16 + 0.10	18208−1306	18 20 50.0	−13 06 01	57.9	+55, +59	11	4.4/11.7	5
18.46 − 0.01	18217−1252	18 21 47.5	−12 52 53	49	+47, +50	23	12.1[16]	9
18.46 − 0.01	18217−1252	18 21 47.5	−12 52 53	49.2	+48, +50	14	12.1[16]	5
18.46 − 0.01	18217−1252	18 21 48.5	−12 52 51	49	+47, +50	23	12.1[16]	4
18.66 + 0.03	18220−1241	18 22 02.5	−12 41 00	80.2	+76, +83	22	5.3/10.8	5
18.88 + 0.05	18224−1228	18 22 24.2	−12 28 54	38.2	+38, +39	3.7	3.3/12.7	5
18.27 − 0.29	18224−1311	18 22 27.1	−13 11 16	75.2	+73, +80	13	5.1/11.0	5
19.47 + 0.17		18 23 07.3	−11 54 30	18	+13, +27	6	1.9/14.2	4
19.49 + 0.15	18232−1154	18 23 12.7	−11 54 16	21	+20, +27	19.3	2.1/13.9	4, 9
19.49 + 0.14	18232−1154	18 23 15.2	−11 54 22	20.7	+18, +25	15	2.1/13.9	5
18.84 − 0.30	18236−1241	18 23 36.0	−12 41 26	41.1	+41, +44	2.3	3.5/12.6[3]	5
18.84 − 0.30	18236−1241	18 23 36.0	−12 41 26	42.0	+39, +45	5	3.5/12.6[3]	3
19.36 − 0.02	18236−1205	18 23 36.3	−12 05 36	26.3	+24, +29	6.7	2.5[20]	5
19.36 − 0.02	18236−1205	18 23 36.3	−12 05 36	27	+24, +31	26	2.5[20]	9
19.61 − 0.12		18 24 26.6	−11 55 18	53		3.6	4.1/11.9	4
19.61 − 0.14	18244−1155	18 24 29.5	−11 55 39	57	+50, +61	18	4.3/11.7	4, 9
19.61 − 0.13	18244−1155	18 24 28.2	−11 55 38	56.3	+48, +58	8.6	4.3/11.7	5
19.62 − 0.23	18248−1158	18 24 49.7	−11 57 52	36	+36, +43	0.4	4.0[16]	4, 9
20.23 + 0.07	18249−1116	18 24 56.9	−11 16 59	72	+60, +78	100	11.1[16]	4
20.24 + 0.07	18249−1116	18 24 57.1	−11 16 42	71.4	+68, +76	94	11.1[16]	5
19.70 − 0.27	18251−1154	18 25 09.2	−11 54 36	43.6	+41, +44	10	3.6/12.4	5
20.08 − 0.14	18253−1130	18 25 23.3	−11 30 44	44		2.9	3.6/12.4	4, 9
19.88 − 0.53	18264−1152	18 26 26.6	−11 52 27	46.8	+46, +47	2.3	3.8/12.2	5
16.87 − 2.16	18265−1517	18 26 32.5	−15 17 58	15	+15, +19	27	2[16]	4, 9
16.87 − 2.16	18265−1517	18 26 32.9	−15 17 51	14.6	+14, +19	23	2[16]	5
17.02 − 2.40	18277−1517	18 27 43.4	−15 16 45	24.1	+20, +25	14	2.0[11]	3
17.01 − 2.40	18277−1517	18 27 42.1	−15 17 17	23.3	+19, +24	3.7	2.0[11]	5
21.56 − 0.03	18278−1009	18 27 49.6	−10 09 19	116.6	+115, +119	14	5.7[20]	5
22.04 + 0.22	18278−0936	18 27 50.0	−09 36 53	53.4	+46, +54	5.5	3.9/11.8	5
21.88 + 0.01	18282−0951	18 28 16.6	−09 51 10	20.4	+20, +22	2.9	1.9/13.8	5
21.88 + 0.01	18282−0951	18 28 16.6	−09 51 10	21	+17, +22	15	1.9/13.8	4, 9
22.35 + 0.05	18290−0924	18 29 01.0	−09 25 15		+79, +81	21.1	5.1/10.6	7
22.35 + 0.05	18290−0924	18 29 01.0	−09 25 15	80	+77, +88	13	5.1/10.6	9
22.35 + 0.05	18290−0924	18 29 01.0	−09 25 15	80	+79, +85	12	5.1/10.6	5
22.43 − 0.16		18 29 57.5	−09 26 41	29	+22, +40	20	2.5/13.2	4
22.43 − 0.23	18302−0928	18 30 12.4	−09 28 46	29.0	+28, +39	3.2	2.5/13.2	5
23.39 + 0.19	18305−0826	18 30 30.4	−08 26 18	74.1	+71, +77	17	4.8/10.8	5
23.81 + 0.39	18305−0758	18 30 35.0	−07 58 00	76.4	+74, +78	9.6	4.9/10.6	5

Table 1 (continued)

Source Name	IRAS Name	R.A. (1950) (h m s)	DEC (1950) (° ′ ″)	$V_{\rm peak}$ (km s^{-1})	$V_{\rm range}$ (km s^{-1})	$S_{\rm peak}$ (Jy)	D (kpc)	Ref.
23.46 + 0.07	18310−0825	18 31 03.6	−08 25 56	87.4	+81, +89	12	5.3/10.3[3]	5
23.46 + 0.07	18310−0825	18 31 03.6	−08 25 56	87	+82, +92	2.3	5.3/10.3[3]	9
23.46 + 0.07	18310−0825	18 31 03.6	−08 25 56	88.4	+85, +90	6	5.3/10.3[3]	3
23.47 + 0.05	18310−0825	18 31 08.2	−08 25 40		+86, +89	11.3	5.3/10.3[3]	7
25.65 + 1.05	18316−0602	18 31 40.0	−06 02 23		+40, +43	113.3	3.3[15]	1
25.65 + 1.05	18316−0602	18 31 38.9	−06 02 08	41.8	+41, +42	181	3.3[15]	3
25.65 + 1.05	18316−0602	18 31 40.0	−06 02 23	41.9	+38, +44	178	3.3[15]	5
25.65 + 1.05	18316−0602	18 31 40.0	−06 02 23	42	+38, +43	105	3.3[15]	9
24.18 − 2.53	18317−0859	18 31 44.8	−08 59 41	75.0	+71, +84	29	4.9/10.8	5
23.25 − 0.24	18317−0845	18 31 45.9	−08 45 47	64.5	+63, +66	8	4.3/11.3[3]	3
23.25 − 0.24	18317−0845	18 31 45.9	−08 45 47	64.1	+63, +65	4.4	4.3/11.3[3]	5
23.25 − 0.24	18317−0845	18 31 45.9	−08 45 47	64	+63, +66	6	4.3/11.3[3]	9
23.25 − 0.24	18317−0845	18 31 46.3	−08 45 39		+62, +66	12.2	4.3/11.3[3]	7
23.01 − 0.41		18 31 55.6	−09 03 09	75	+69, +84	405	4.9/10.8	4
23.44 − 0.18	18319−0834	18 31 55.3	−08 34 01	103	+94, +113	77	9.0[9]	4, 9
23.44 − 0.18	18319−0834	18 31 55.3	−08 34 01	102.6	+95, +108	40	9.0[9]	5
23.16 − 0.38	18321−0854	18 32 07.0	−08 54 06	81.8	+72, +83	12	5.2/10.5	5
23.32 − 0.30	18321−0843	18 32 07.3	−08 43 36	63.8	+63, +76	2.2	4.4/11.2	5
23.66 − 0.13	18321−0820	18 32 08.5	−08 20 46	82.1	+76, +87	11	5.2/10.4	5
24.54 + 0.31	18322−0721	18 32 13.5	−07 21 42	106.2	+103, 111	15	6.3/9.2	5
23.19 − 0.50	18324−0855	18 32 26.4	−08 55 02	75.2	+73, +83	9.2	4.9/10.7	5
23.70 − 0.19	18324−0820	18 32 27.3	−08 20 23	80.0	+75, +81	30	4.9/10.6[3]	3, 7
23.70 − 0.19	18324−0820	18 32 27.3	−08 20 23	79.0	+75, +85	9.2	4.9/10.6[3]	5
23.70 − 0.19	18324−0820	18 32 27.3	−08 20 23	78	+58, +81	26	4.9/10.6[3]	9
24.33 + 0.15	18324−0737	18 32 35.2	−07 37 33	109.9	+107, +120	4.6	6.5/9.0	5
24.49 − 0.04	18334−0733	18 33 23.3	−07 33 50		+113, +116	33.1	6.6/8.9[3]	1
24.49 − 0.04	18334−0733	18 33 23.3	−07 33 50	115.2	+114, +116	29	6.6/8.9[3]	3
24.49 − 0.04	18334−0733	18 33 23.3	−07 33 50	114.4	+108, +116	29	6.6/8.9[3]	5
24.79 + 0.08		18 33 29.9	−07 14 45	114	+105, +115	82	6.8/8.7	4
24.81 + 0.10	18335−0713	18 33 30.1	−07 13 10	113.0	+106, +115	97	6.7/8.7	5
24.85 + 0.09	18335−0711	18 33 35.1	−07 11 33	110	+109, +115	21	6.5/8.9	4, 9
22.92 + 0.08	18337−0707	18 33 45.9	−07 07 46	109.3	+107, +118	13	6.5/8.9	5
24.68 − 0.16	18341−0727	18 34 09.3	−07 27 23	114.0	+113, +115	16	6.6/8.9[3]	3
24.68 − 0.16	18341−0727	18 34 09.3	−07 27 23	113.1	+111, +114	3.5	6.6/8.9[3]	5
25.41 + 0.10	18345−0641	18 34 36.9	−06 41 15	94.7	+93, +100	8.0	5.7/9.6	5
25.41 + 0.10	18345−0641	18 34 36.9	−06 41 15		+94, +100	34.8	5.7/9.6	1
25.70 + 0.03	18353−0628	18 35 23.8	−06 28 07	96	+89, +101	225	14.0[9]	5, 9
26.60 − 0.02	18372−0541	18 37 15.7	−05 41 37	24.6	+17, +25	13	2.0/13.2	5
26.65 + 0.02	18372−0537	18 37 12.4	−05 37 55	107.1	+106, +108	5.9	6.5/8.7	5
26.61 − 0.21	18379−0546	18 37 57.4	−05 46 11	104.2	+103, +116	9	6.1/9.1[3]	3
26.61 − 0.21	18379−0546	18 37 57.4	−05 46 11	103.2	+102, +115	19	6.1/9.1[3]	5
26.61 − 0.22	18379−0546	18 37 58.2	−05 46 28		+102, +105	10.0	6.1/9.1[3]	1
27.30 + 0.15	18379−0500	18 37 55.5	−05 00 34	34.9	+34, +37	21	7.8[16]	5
27.30 + 0.15	18379−0500	18 37 55.5	−05 00 34	34.9	+34, +36	41	7.8[16]	3
27.36 − 0.16	18391−0504	18 39 11.0	−05 04 43	99.7	+91, +102	23	6.1/9.0	5
27.36 − 0.16	18391−0504	18 39 11.0	−05 04 43	100	+88, +104	29	6.1/9.0	4
27.79 + 0.04	18392−0436	18 39 15.8	−04 36 09	111.8	+108, +113	1.9		5
28.15 + 0.00		18 40 02.2	−04 28 16	101	+92, +105	34	6.0/9.0	4
28.40 + 0.07	18402−0403	18 40 16.5	−04 03 14	71.1	+67, +81	3.4	4.6/10.4	5
28.20 − 0.05	18403−0417	18 40 19.3	−04 17 02	100.8	+94, +104	56	6.2/8.7	5
28.20 − 0.05	18403−0417	18 40 19.3	−04 17 02	99	+94, +102	3.3	6.2/8.7	4, 9
28.86 + 0.07	18411−0338	18 41 07.9	−03 38 36	105		1.1	6.7/8.2	4, 9
28.29 − 0.38	18416−0420	18 41 39.8	−04 21 00	81.5	+81, +84	75	5.0/10.0[3]	3
28.29 − 0.38	18416−0420	18 41 39.8	−04 21 00	82	+40, +95	62	5.0/10.0[3]	9
28.29 − 0.38	18416−0420	18 41 39.8	−04 21 00	80.7	+79, +93	62	5.0/10.0[3]	5
28.31 − 0.40	18416−0420	18 41 45.8	−04 20 52		+80, +84	58.6	5.0/10.0[3]	7
28.84 − 0.23	18421−0348	18 42 09.5	−03 47 58	100	+99, +104	1.3	6.3[16]	4

Table 1 (continued)

Source Name	IRAS Name	R.A. (1950) ($^{h\ m\ s}$)	DEC (1950) ($^{\circ\ \prime\ \prime\prime}$)	$V_{\rm peak}$ (km s^{-1})	$V_{\rm range}$ (km s^{-1})	$S_{\rm peak}$ (Jy)	D (kpc)	Ref.
28.83 − 0.24	18421−0348	18 42 11.3	−03 48 37	83.9	+81, +93	58	6.3[16]	5
28.83 − 0.25	18421−0348	18 42 13.1	−03 49 01	83	+79, +94	73	6.3[16]	4
29.86 − 0.05		18 43 22.9	−02 48 26	101	+99, +105	67	6.5/8.2	4
29.94 − 0.02	18434−0242	18 43 25.6	−02 43 22	100.4		23	9.0[9]	4
29.95 − 0.02	18434−0242	18 43 26.7	−02 42 38	96	+95, +102	206	9.0[9]	4, 9
29.98 − 0.04		18 43 34.9	−02 42 19	104	+97, +105	14	7.0/7.7	4
30.30 + 0.06	18438−0222	18 43 48.9	−02 22 28	36.7	+32, +51	11	2.7/12.0	5
30.82 + 0.27	18440−0148	18 44 00.6	−01 48 41	104.9	+104, +111	3.0	8.2[16]	5
30.82 + 0.27	18440−0148	18 44 00.6	−01 48 41	105	+100, +111	8	8.2[16]	4, 9
30.78 + 0.23		18 44 05.7	−01 51 48	49	+47, +49	24	3.4/11.2	4
30.76 + 0.21	18441−0153	18 44 08.4	−01 53 42	48.9	+47, +49	19	3.4/11.2	5
30.76 + 0.21	18441−0153	18 44 08.4	−01 53 42	87.5	+76, +88	8.2	5.6/9.0	5
31.05 + 0.35	18441−0134	18 44 08.8	−01 34 12	80.8	+78, +84	4.5	5.2/9.4	5
30.79 + 0.20		18 44 12.3	−01 52 04	86	+75, +89	23	5.5/9.1	4
30.23 − 0.13	18443−0231	18 44 21.7	−02 31 12	108.1	+100, +114	18	6.0/8.7	5
30.54 + 0.02	18443−0210	18 44 23.9	−02 10 44	53	+52, +54	0.6	13.8[9]	9
30.20 − 0.17		18 44 25.8	−02 33 57	108	+101, +111	18.7	7.1/7.6	4
30.22 − 0.18		18 44 31.3	−02 32 50	113	+111, +115	11.7		4
30.86 + 0.12	18446−0150	18 44 38.1	−01 50 33	102	+37, +108	2.4	7.6/9.1[9]	9
30.91 + 0.14	18446−0150	18 44 38.2	−01 47 34		+98, +111	53.6	7.6/9.1[9]	7
30.58 − 0.04	18446−0209	18 44 41.2	−02 09 42	42.4	+40, +48	4.8	3.2[14]	5
30.59 − 0.04	18446−0209	18 44 42.5	−02 09 43	43	+36, +49	7.5	3.2[14]	4
30.82 − 0.05		18 45 10.5	−01 57 46	101	+91, +110	18	6.9/7.7	4
31.07 + 0.08	18452−0141	18 45 10.0	−01 40 41		+15, +17	13.4	1.3/13.3	7
31.07 + 0.05	18452−0141	18 45 15.5	−01 41 35	16	+15, +17	3	1.3/13.3	5, 9
30.87 − 0.10	18454−0156	18 45 26.6	−01 56 08	101.1	+101, +108	4.3	6.9/7.7	5
31.16 + 0.04	18454−0136	18 45 28.1	−01 36 46	40.8	+40, +48	2.9	2.9/11.6	5
30.99 − 0.08	18455−0149	18 45 35.0	−01 49 03	74.7	+73, +78	5.9	4.8/9.8	5
31.28 + 0.06	18456−0129	18 45 37.2	−01 30 00	110.0	+102, +113	71	7.3[16]	5
31.28 + 0.06	18456−0129	18 45 37.2	−01 30 00	110	+102, +114	81	7.3[16]	4, 9
31.58 + 0.08	18461−0113	18 46 06.8	−01 13 38	98.4	+95, +100	5.6	6.7/7.7	5
32.03 + 0.05	18470−0050	18 47 01.9	−00 50 21	92.8	+92, +102	93	6.1/8.3	5
32.11 + 0.99	18470−0044	18 47 02.1	−00 44 35	93.2	+91, +105	31	6.2/8.2	3
32.03 + 0.05	18470−0049	18 47 03.8	−00 48 59		+91, +102	103.6	6.6/7.8	1
32.74 − 0.08	18487−0015	18 48 47.8	−00 15 50	38.2	+28, +39	48	2.0/12.0[18]	5
32.74 − 0.08	18487−0015	18 48 47.8	−00 15 50	39	+24, +45	47	2.0/12.0[18]	4
32.99 + 0.04	18488+0000	18 48 51.1	00 00 41	92.6	+90, +94	21	6.0/8.3[3]	3
32.99 + 0.04	18488+0000	18 48 51.1	00 00 41	91.7	+89, +93	27	6.0/8.3[3]	5
32.99 + 0.03	18488+0000	18 48 54.1	00 00 36		+89, +93	16.3	6.0/8.3[3]	1
33.09 − 0.07	18494+0002	18 49 25.1	00 02 51	104.6	+95, +106	19	5.7/8.5	5
33.09 − 0.07	18494+0002	18 49 25.1	00 02 51	96	+95, +106	30	5.7/8.5	4
33.13 − 0.09	18496+0004	18 49 33.6	00 04 25	73.5	+72, +75	13	7.1[16]	5
33.13 − 0.09	18496+0004	18 49 33.6	00 04 25	73	+71, +81	12.4	7.1[16]	4
33.42 − 0.00	18497+0022	18 49 47.0	00 22 07	105.0	+100, +108	26	9.5[16]	3
33.42 − 0.00	18497+0022	18 49 47.0	00 22 07	105.0	+96, +107	20	9.5[16]	5
34.25 + 0.15	18507+0110	18 50 46.6	01 11 06	57.9	+55, +63	18	3.8[16]	5
34.25 + 0.15	18507+0110	18 50 47.0	01 10 49	58	+58, +62	29	3.8[16]	4
34.40 + 0.23	18507+0121	18 50 45.2	01 21 09	55.8	+55, +63	27	3.6[15]	5
34.39 + 0.21	18507+0121	18 50 48.5	01 19 48		+55, +64	18.5	3.6[15]	7
34.24 + 0.13		18 50 49.0	01 09 57	55.5	+55, +62	20	3.8/10.3	4
34.00 − 0.01	18508+0052	18 50 52.7	00 52 40	59.0	+58, +63	3.9	4.0/10.1	5
33.70 − 0.26	18512+0029	18 51 13.0	00 29 45	62.6	+58, +64	68	4.2/10.0	5
35.02 + 0.35	18515+0157	18 51 29.0	01 57 29	44.1	+40, +47	56	3.6[16]	4
35.02 + 0.35	18515+0157	18 51 29.0	01 57 29	44	+40, +47	35	3.6[16]	5
37.43 + 1.50	18517+0437	18 51 48.7	04 37 19		+40, +52	298	2.9/10.6	7
37.43 + 1.52	18517+0437	18 51 45.3	04 37 42	41.1	+40, +52	279	2.9/10.6	5
36.12 + 0.55	18527+0301	18 52 46.2	03 01 13	73.0	+70, +85	19	5.0/8.7	5

Table 1 (continued)

Source Name	IRAS Name	R.A. (1950) (h m s)	DEC (1950) (° ′ ″)	$V_{\rm peak}$ (km s^{-1})	$V_{\rm range}$ (km s^{-1})	$S_{\rm peak}$ (Jy)	D (kpc)	Ref.
35.20 − 0.74	18556+0136	18 55 41.1	01 36 26	28	+26, +35	125	2.1/11.8[18]	4
35.20 − 0.74	18556+0136	18 55 41.1	01 36 26	28.9	+26, +37	64	2.1/11.8[18]	5
37.55 + 0.20	18566+0408	18 56 40.8	04 08 03	84.2	+76, +88	4	6.3/7.2[3]	3
37.55 + 0.20	18566+0408	18 56 40.8	04 08 03	83.7	+78, +87	6.6	6.3/7.2[3]	5
34.80 − 1.38	18572+0057	18 57 14.9	00 57 38		+43, +48	20.8	10.7[16]	1
34.80 − 1.40	18572+0057	18 57 16.2	00 57 21	47.5	+42, +48	27	10.7[16]	3
34.80 − 1.40	18572+0057	18 57 16.2	00 57 21	46.9	+43, +48	31	10.7[16]	5
37.54 − 0.11	18577+0358	18 57 46.5	03 58 52	62.6	+49, +63	5.7	4.3/9.1	5
35.20 − 1.74	18592+0108	18 59 13.1	01 09 07	42	+39, +47	560	3.0[16]	4
35.20 − 1.74	18592+0108	18 59 14.5	01 08 46	42.6	+40, +47	595	3.0[16]	5
38.12 − 0.22	18592+0426	18 59 14.3	04 26 24	69.4	+69, +71	2.3	4.9/8.5	5
40.42 + 0.70	19002+0654	19 00 13.5	06 54 37	15.6	+5, +16	18	1.2/11.8	5
40.42 + 0.70	19002+0654	19 00 14.4	06 54 28		+13, +17	12.6	1.2/11.8	7
38.93 − 0.37	19012+0505	19 01 15.5	05 05 19	32.3	+31, +34	5.4	2.3/10.9	5
40.27 − 0.20	19031+0621	19 03 09.8	06 21 31	74.0	+64, +81	18	6.2/6.8	5
40.62 − 0.14	19035+0641	19 03 34.6	06 41 57	31.0	+30, +36	15	10.5[16]	5
40.62 − 0.14	19035+0641	19 03 34.6	06 41 57	31	+30, +37	17	10.5[16]	4
41.11 − 0.24	19048+0705	19 04 51.1	07 05 17	63.4	+63, +64	3.7	4.7/8.1	5
41.23 − 0.19	19049+0712	19 04 55.4	07 12 40	57.1	+55, +58	3.2	4.2/8.6	5
43.15 + 0.02		19 07 47.0	09 00 30	13		26		4
43.16 + 0.02	19078+0901	19 07 48.3	09 01 18	9.1	+7, +22	31	14.0[16]	5
43.16 + 0.02	19078+0901	19 07 48.3	09 01 18	9	+8, +20	22	14.0[16]	4
43.17 + 0.01	19078+0901	19 07 51.0	09 01 21	20.0	+19, +22	12.8	14.0[16]	4
43.17 − 0.00	19078+0901	19 07 52.6	09 01 04	−1		3.4	14.0[16]	4
43.03 − 0.45	19092+0841	19 09 13.4	08 41 27	54.8	+54, +57	10	4.2/8.1	5
43.80 − 0.13	19095+0930	19 09 30.7	09 30 42	40	+39, +44	144	3.4[16]	4
43.80 − 0.13	19095+0930	19 09 30.7	09 30 42	39.5	+39, +44	79	3.4[16]	5
43.18 − 0.52	19097+0847	19 09 44.8	08 47 09	58.8	+58, +60	5.5	4.6/7.8	5
45.07 + 0.13	19110+1045	19 11 00.5	10 45 41	58	+57, +60	33	8.3[16]	4
45.07 + 0.13	19110+1045	19 11 00.5	10 45 41	57.8	+57, +59	45	8.3[16]	5
45.47 + 0.13	19117+1107	19 11 46.2	11 07 03	65	+59, +74	7	9.5[16]	4
45.47 + 0.13	19117+1107	19 11 46.2	11 07 03	65.8	+57, +67	10	9.5[16]	5
45.49 + 0.13		19 11 50.0	11 07 53	57.2		13.4	4.9/7.0	4
45.44 + 0.07		19 11 56.6	11 03 44	50		1.9	4.0/8.0	4
43.89 − 0.78	19120+0917	19 12 02.8	09 17 19	47.4	+47, +53	34	3.6/8.7	5
43.89 − 0.78	19120+0917	19 12 03.1	09 17 38		+47, +52	9.8	3.6/8.7	7
45.46 + 0.06	19120+1103	19 12 00.4	11 03 59	56.1	+55, +66	4.1	6.0[18]	5
45.47 + 0.05	19120+1103	19 12 02.5	11 04 31	56	+55, +59	5.3	6.0[18]	4
49.41 + 0.33	19186+1440	19 18 39.7	14 40 58	−12.4	−27, −10	13	12.1	5
50.01 + 0.59	19189+1520	19 18 55.0	15 20 16	−5.0	−10, −2	6.5	11.3	5
50.32 + 0.68	19191+1538	19 19 11.4	15 38 37	29.9	+26, +33	2.8	2.5/8.4	5
49.57 − 0.27	19211+1432	19 21 10.4	14 32 19	62.8	+58, +66	29	17.7	5
49.47 − 0.37		19 21 20.6	14 24 16	64	+60, +75	12	7.6[16]	4
49.49 − 0.37	19213+1424	19 21 21.8	14 25 08	56		33	7.6[16]	4
49.49 − 0.39		19 21 25.7	14 24 42	59	+51, +60	850		4
49.59 − 0.39	19216+1429	19 21 37.2	14 29 52	59.3	+51, +62	480	17.4	5
49.67 − 0.46	19220+1432	19 22 02.2	14 32 07	59.6	+51, +61	10	4.5[3]	3
49.05 − 1.09	19230+1341	19 23 06.9	13 41 41		+33, +38	24.3	2.9/8.2	1
49.05 − 1.09	19230+1341	19 23 06.9	13 41 41	35.5	+34, +41	21	2.9/8.2	5
53.03 + 0.12	19266+1745	19 26 40.1	17 45 41	10.0	+9, +11	3.3	0.8/9.4	5
53.14 + 0.07	19270+1750	19 27 03.9	17 50 04	23.8	+23, +25	1.9	1.7/8.5	5
53.63 + 0.02	19282+1814	19 28 14.7	18 14 32	18.7	+18, +19	6.3	1.6/8.5	5
52.67 − 1.09	19303+1651	19 30 20.2	16 51 04		+64, +68	10.0	16.2	2
58.77 + 0.65	19366+2301	19 36 40.1	23 01 42	34.0	+31, +36	2.8	11.6	5
59.83 + 0.67	19388+2357	19 38 52.6	23 57 36	38.4	+36, +41	31	2.7[3]	3
59.84 + 0.66	19388+2357	19 38 55.9	23 57 50		+37, +39	24.7	2.7[3]	7
59.78 + 0.06	19410+2336	19 41 03.6	23 36 51	17.3	+14, +28	34	1.8/6.8	5
59.78 + 0.06	19410+2336	19 41 03.6	23 36 51	25	+14, +27	42	2.9/5.7	4

Table 1 (continued)

Source Name	IRAS Name	R.A. (1950) ($^{\rm h}$ $^{\rm m}$ $^{\rm s}$)	DEC (1950) ($^\circ$ $'$ $''$)	$V_{\rm peak}$ (km s^{-1})	$V_{\rm range}$ (km s^{-1})	$S_{\rm peak}$ (Jy)	D (kpc)	Ref.
60.57 − 0.19	19437+2410	19 43 45.4	24 10 18	3.6	+3, +4	4.1	0.3/8.0	5
70.14 + 1.73	19589+3320	19 58 57.0	33 20 47	−26.4	−30, −22	22	8.0[16]	3
70.14 + 1.73	19589+3320	19 58 57.0	33 20 47	−26.5	−27, −26	9.8	8.0[16]	5
73.06 + 1.80	20062+3550	20 06 17.1	35 50 32	−2.8	−4, −2	32	5.7[3]	3
73.06 + 1.80	20062+3550	20 06 17.1	35 50 32	−2.5	−4, +7	10	5.7[3]	5
69.54 − 0.98	20081+3122	20 08 09.9	31 22 42	15.1	0, +16	109	1.4[16]	5
71.53 − 0.40	20110+3321	20 11 05.1	33 21 11	10.7	+3, +11	5.3	2.3/3.1	5
78.12 + 3.63	20126+4104	20 12 41.0	41 04 20	−6.1	−8, −5	38	1.7[16]	5
78.12 + 3.63	20126+4104	20 12 41.0	41 04 20	−6.5	−8, −4	61	1.7[16]	3
75.77 + 0.34	20198+3716	20 19 49.1	37 16 16	−2.9	−11, +1	39	3.9[16]	5
79.75 + 0.99	20290+4052	20 29 03.1	40 52 16		−6.5, −3	26.5	3.9	2
80.87 + 0.42	20350+4126	20 35 04.8	41 26 02	−4.1	−5, −4	4.3	4.8[18]	5
80.87 + 0.42	20350+4126	20 35 04.8	41 26 02	−4.0	−6, −3	10	4.8[18]	3
99.92 + 1.51	21074+4949	21 07 28.4	49 49 46	−70.5	−72, −68	27	9.3	5
94.60 − 1.80	21381+5000	21 38 10.6	50 00 42	−40.9	−44, −40	7.0	6.0[16]	5
94.60 − 1.80	21381+5000	21 38 10.6	50 00 42	−43.9	−45, −39	19	6.0[16]	3
98.04 + 1.45	21413+5442	21 41 21.2	54 42 30	−61.6	−62, −61	3.3	7.5[18]	5
108.19 + 5.52	22272+6358	22 27 12.2	63 58 21	−10.9	−13, −9	91	0.9[16]	5
108.19 + 5.52	22272+6358	22 27 12.2	63 58 21	−11.3	−12, −10	109	0.9[16]	3
109.87 + 2.12	22543+6145	22 54 20.2	61 45 55	−2.5	−5, −1	815	0.7[11]	5
109.92 + 1.98	22551+6139	22 55 11.7	61 40 00	−2.4	−6, −1	43	0.6[3]	3
108.76 − 0.95	22566+5830	22 56 37.0	58 30 52	−45.7	−46, −45	2.8	5.3[14]	5
111.54 + 0.78	23116+6111	23 11 36.0	61 11 49	−56.3	−62, −48	296	2.8[16]	5
111.25 − 0.77	23139+5939	23 13 58.3	59 39 06	−38.5	−42, −37	4.0	3.5[16]	5

References for sources and distances:
1 van der Walt et al. 1995. 2 van der Walt et al., 1996.
3 Slysh et al., 1999. 4 Caswell et al., 1995. 5 Szymczak et al., 2000.
6 MacLeod et al., 1992. 7 Schutte et al., 1993. 8 Gaylard et al. 1993.
9 Walsh et al., 1997. 10 Caswell et al., 1996. 11 Wu et al., 1996.
12 Humphreys, 1978. 13 Eiroa et al., 1994. 14 Wouterloot et al., 1993.
15 Palla et al., 1991. 16 Larionov et al., 1999. 17 Hughes & MacLeod, 1993.
18 Baudry et al., 1997. 19 Jijina et al., 1999. 20 Molinari et al., 1996.

(upper panel) encloses the region $[25-12] > 0.57$ and $[60-12] > 1.30$, first defined by Wood and Churchwell (1989, hereafter the WC criterion) and is often used to identify massive stars associated with UC HII regions. Only about 13% (48/361) lie outside the box. Methanol maser emission is believed to be associated with massive stars, and so the WC criterion receives further support here. It is noteworthy that although the objects, taken as a whole, have a large spread in the color-color diagram, more than 70% (219/361) fall inside a very small region: $0.57 \le [25-12] \le 1.30$ and $1.30 \le [60-12] \le 2.50$ (the central box). The distribution in the color-color diagram might indicate an evolutionary phase of star formation since the IRAS colors are possibly related to the evolution of the 6.7 GHz methanol sources (MacLeod et al. 1998). Maser will not be excited if the radiation is too weak, and will be destroyed if the radiation becomes too strong. In the earliest stage of star formation, the massive star is surrounded by cold and dark clouds with very red IRAS colors. The emission of dust from the circumstellar disk or envelope is too weak to produce the 6.7 GHz methanol maser emission efficiently. With the appearance of an UC HII region, the emission of dust gets stronger and also the maser emission. At that time, the radio continuum from the UC HII region is too small and/or weak to be detected (Walsh et al. 1998, 2001; De Buizer et al. 2000; Lee et al. 2001; Minier et al. 2001). As the UC HII evolving further, however, the masing gas cloud either warms up or is destroyed by the expanding UC HII region. Therefore, the fact that the majority is located in a small region in the color-color diagram indicates that the 6.7 GHz methanol maser appears only within a very short period during the earliest stage of star formation. The dotted line (lower panel) in the color-color plot is the best fit, which possibly indicates an evolutionary trend of maser frequency as one moves along this line from the top right corner (very red colors) to the bottom left corner (very blue colors).

3.4 Velocity Range of Maser Emission

The 6.7 GHz methanol maser emission has a large velocity dispersion ranging from less than 0.5 to 71 km s^{-1}, as shown in Fig. 3. The mean velocity range is about 8.2 km s^{-1}. This appears to be consistent with the result of Slysh et al. (1999). Apparently the velocity ranges belong to two groups: one from 1 to 10 km s^{-1} (peaking at 5) one from about 11 to 20 km s^{-1} (peaking at 12). Nearly 62% (298/482) belong to the first group, and about 36% (138/482) to the second group. Only a few objects are outside these two groups. Among the outsiders, three have ranges greater than 30 km s^{-1} (the largest one is 71 km s^{-1} for the source 18446–0150).

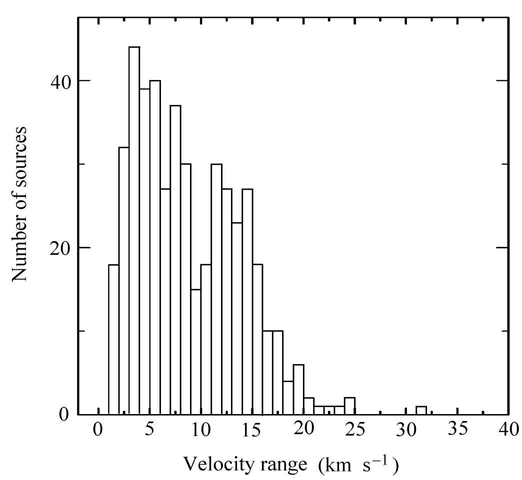

Fig. 3 Velocity range distribution of 6.7 GHz methanol masers. The velocity range is less than 20 km s^{-1} for most objects. A few have ranges greater than 30 km s^{-1}, and the largest range is 71 km s^{-1}.

The velocity range can be caused by different masers with different radial velocities. The 6.7 GHz methanol masers may stem from different directions because masers can in principle occur in either outflows or disks (Sobolev et al. 1997; Norris et al. 1993, 1998; Walsh et al. 1998, 2001; De Buizer et al. 2000; Lee et al. 2001; Minier et al. 2000, 2001), and in general the velocity range can be very different for masers from outflows and disks. If the masers occur in the disk, then their velocities will be close to the Keplerian velocities, and a small velocity range will be expected; but if they occur in outflows then a larger velocity range will result since they may stem from different directions. When an outflowing wind strikes a denser material a low-velocity maser may be produced, whereas if the wind strikes a less dense material a higher-velocity maser will be expected. Therefore, there may exist a large velocity spread if the 6.7 GHz methanol masers originate from outflows.

An alternative explanation for the double-peak of the velocity range distribution could be that the masers in the first group originate from circumstellar disks while the second group comes from outflows.

For the first group, the Keplerian velocity of a maser is about 3 km s^{-1}, assuming the mass of the young star, $\sim$ 10 $M_{\odot}$, and the maser at a distance of 1000 AU (Slysh et al. 1999). To some extent, there are uncertainties in the distance and the mass, so the observed peak at about twice this value can be considered as consistent with this interpretation.

The 6.7 GHz methanol masers in the second group lie probably in outward-propagating shocks. The gas within circumstellar envelopes heated by the central star will be at a much higher pressure than the surrounding cool gas, and will tend to expand. Since the expansion velocity is likely to exceed the sound velocity in the surrounding gas region, a shock front may be expected to form, moving out through the ambient gas. This is similar to the 'expanding shock' (Walsh et al. 1998). The Keplerian velocity and the expansion velocity of masers may each be about a few km s^{-1}; together, they could result in a range of about 10–20 km s^{-1} or more, as is observed for the second group. The few objects with velocity ranges more than 30 km s^{-1} are likely to originate from high-velocity outflows. For example, some maser components in W 75 may originate from a jet (Minier et al. 2001).

3.5 Relations between Maser and Infrared Flux Densities, and between Maser and Infrared Luminosities

We have investigated the relations between the 6.7 GHz methanol maser peak flux density and the IRAS flux densities in four IRAS bands for the 361 sources (Fig. 4). Except for a few objects, the maser flux density is less than 20 percent of the 60 μm flux density and less than 25 per cent of the 100 μm flux density. This appears to be consistent with the results obtained by van der Walt et al. (1995), Slysh et al. (1999), and Szymczak & Kus (2000). Some significant correlations were found between the maser peak flux density and the 25, 60, and 100 μm flux densities: the respective correlation coefficients are 0.19 at 99.97% at confidence level, 0.23 at 99.99%, and 0.22 at 99.99%. This means that the maser peak flux density increases with the 25, 60, and 100 μm flux densities. This is inconsistent with the results of van der Walt et al. (1995) and Szymezak & Kus (2000) who found only weak or no correlation between them. Although some clear cases of correlation are found, the scatter in both axes is several decades, so it is unclear whether or not there is real physical connection between the them. No correlation was found between the maser peak flux density and the 12 μm flux density, in agreement with what was first noted by van der Walt et al. (1995).

We plot the 6.7 GHz methanol maser luminosity against the corresponding infrared luminosity for 355 sources in Fig. 5. The infrared luminosity is calculated with the formula of Casoli et al. (1986). From the plot, we can see that the 6.7 GHz methanol luminosity increases with the infrared luminosity. The correlation coefficient is 0.34 at 99.99% confidence level.

The infrared emission is predominantly produced by circumstellar dust that has been heated by the central star, while the maser emission is produced by some clumps or inhomogeneities inside some circumstellar envelope or disk. Therefore, the infrared emission originates from a much larger region than does the maser emission. Now, the dust grain temperature decreases

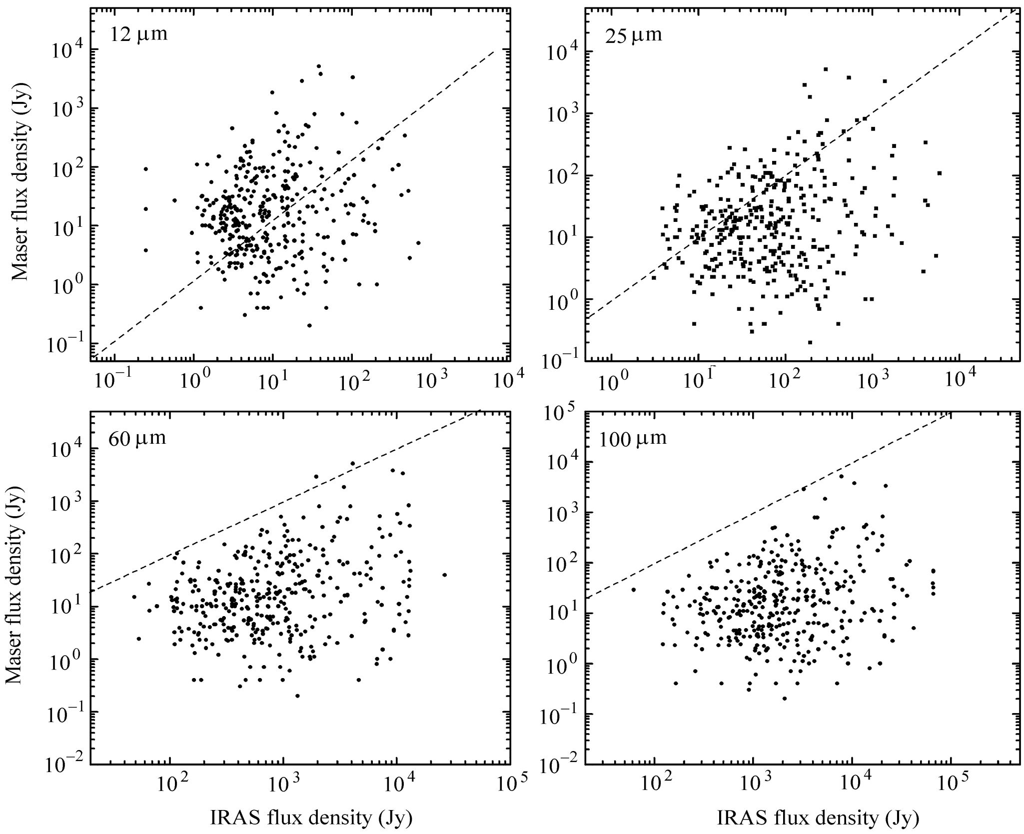

Fig. 4 The 6.7 GHz maser peak flux density versus IRAS flux densities. Equality of the two is marked by the dashed line.

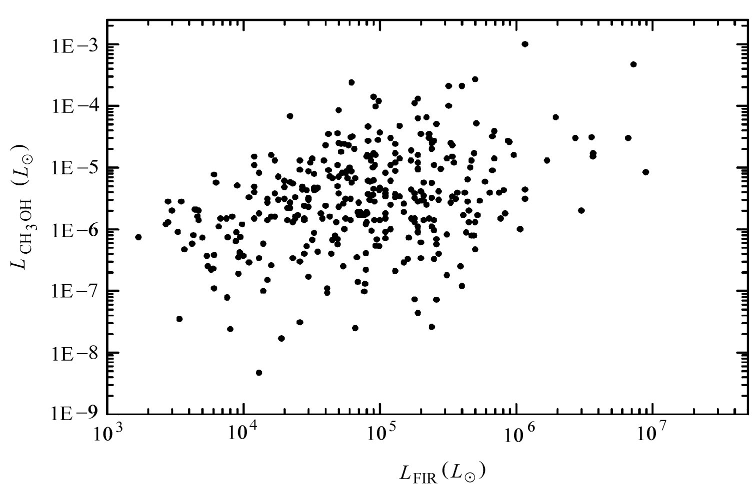

Fig. 5 Methanol maser luminosity (L_{CH_3OH}) versus the associated infrared source luminosity (L_{FIR}). The correlation coefficient is 0.34 at confidence level 99.99%.

with increasing distance from the central star because of the increased dilution of the stellar radiation field and the decreased ability of the dust to absorb the increasingly longer wavelength radiation. The radiation, at 12 μm, is generally attributed to emission from grains of the inner circumstellar envelope or disk (perhaps within the HII region), where the radiation is too strong to produce the 6.7 GHz methanol maser emission (either there is not enough methanol molecular to form the maser or the gas temperature so high as to quench the maser), while the radiation at 25 to 100 μm originates from a larger distance, where the conditions may be right for masing. On the other hand, the fact that in most of the methanol sources, the maser flux density is less than 20 percent of the far-infrared flux densities suggests that the far-infrared radiation is a possible maser pump. This is also suggested by the fact that most of the stellar luminosity is attributed to the far-infrared radiation. For if this is true, then the maser intensity will depend on the far-infrared flux densities, which has indeed been shown by the correlation to varying degree between the maser peak flux density and the 25, 60, and 100 μm flux densities. These correlations, therefore, manifest that the maser emission is in fact associated with the far-infrared emission from the dust at a larger distance from the star. In short, the 6.7 GHz methanol masers most probably originate from outer molecular envelopes or disks.

4 SUMMARY

From a statistical study of all the known 6.7 GHz methanol maser sources, we obtain the major findings as follows.

(1) On the color-color diagram, more than 70% objects fall within a very small region with $0.57 \leq [25-12] \leq 1.30$ and $1.30 \leq [60-12] \leq 2.50$, suggesting that the 6.7 GHz methanol maser emission may appear only during a limited period of massive star formation.

(2) The velocity ranges of masers consist of two main groups: one from 1 to 10 km s^{-1}, and one from about 11 to 20 km s^{-1}, which indicates that the masers may be associated with both disks and outflows.

(3) Some significant correlations are found between the maser and far-infrared flux densities, and between the maser and infrared luminosities: the maser peak flux density is proportional to the 25, 60, and 100 μm flux densities, respectively; and the maser luminosity increases with the far-infrared luminosity. These correlations suggest that the far-infrared radiation is a possible pumping mechanism for the 6.7 GHz methanol masers which most probably originate from outer molecular envelopes or disks.

Acknowledgements This work was supported by the National Natural Science Foundation of China, under Grant Nos. 19973017 and 10103003.

References

Beudry A., Desmurs J. F., Wilson T. L. et al., 1997, A&A, 325, 255
Caswell J. L., Vaile R. A., Ellingsen S. P. et al., 1995, MNRAS, 272, 96
Caswell J. L., 1996, MNRAS, 283, 606
Casoli F., Dupraz C., Gerin M. et al., 1986, A&A, 169, 281
Dame T. M., Hartmann D., Thaddeus P., 2001, ApJ, 547, 792
De Buizer J. M., Piã R. K., Telesco C. M., 2000, ApJS, 130, 437
Eiroa C., Casali M. M., Miranda L. F. et al., 1994, A&A, 290, 599
Ellingsen S. P., von Bibra M. L., McCulloch P. M. et al., 1996a, MNRAS, 280, 378

Gaylard M. J., MacLeod G. C., 1993, MNRAS, 262, 43
Hughes V A., MacLeod G. C., 1993, AJ, 105, 1495
Humphreys R. H., 1978, ApJS, 38, 309
Jijina J., Myers P. C., Adams F. C., 1999, ApJS, 125, 161
Larionov G. M., Val'tts I. E., Winnberg A. et al., 1999, A&AS, 139, 257
Lee J. K., Walsh A. J., Burton M. G. et al., 2001, MNARS, 324, 1102
Lyder D. A., Galt J., 1997, AJ, 113, 1310
MacLeod G. C., Gaylard M. J., 1992, MNRAS, 256, 519
MacLeod G. C., Gaylard M. J., Nicolson G. D., 1992, MNRAS, 254, 1p
MacLeod G. C., van der Walt D. J., North A. et al. 1998, AJ, 116, 2936
MacLeod G. C., Gaylard M. J., 1992, MNRAS, 256, 519
Menten K. M., 1991, ApJ, 380, L75
Minier V., Booth R. S., Conway J. E., 2000, A&A, 362, 1093
Minier V., Conway J. E., Booth R. S., 20001, A&A, 369, 278
Molinari S., Brand J., Cesaroni R., Palla F., 1996, A&A, 308, 573
Norris R. P., Whiteoak J. B., Caswell J. L. et al., 1993, ApJ, 412, 222
Norris R. P., Byleveld S. E., Diamond P. J. et al., 1998, ApJ, 508, 275
Palla F., Brand J., Cesaroni R. et al., 1991, A&A, 246, 249
Schutte A. J., van der Walt D. J., Gaylard M. J., MacLeod G. C., 1993, MNRAS, 261, 783
Slysh V. I., Val'tts I. E., Kalenskii S. V. et al., 1999, A&AS, 134, 115
Sobolev A. M., Cragg D. M., Godfrey P. D., 1997, A&A, 324, 211
Szymczak M., Kus A. J., 2000, A&AS, 147, 181
van der Walt D. J., Gaylard M. J., MacLeod G. C., 1995, A&AS, 110, 81
van der Walt D. J., Retief S. J. P., Gaylard M. J. et al., 1996, MNRAS, 282, 1085
Walsh A. J., Hyland A. R., Robinson G., Burton M. G., 1997, MNRAS, 291, 261
Walsh A. J., Burton M. G., Hyland A. R., Robinson G., 1998, MNRAS, 301, 640
Walsh A. J., Bertoldi F., Burton M. G. et al., 2001, MNRAS, 326, 36
Wood D. O. S., Churchwell E., 1989, ApJ, 340, 265 (WC)
Wouterloot J. G. A., Brand J., 1989, A&AS, 80, 149
Wouterloot J. G. A., Brand J., Fiegle K., 1993, A&AS, 98, 589
Wu Y., Huang M., He J. et al., 1996, A&AS, 115, 283